Research Square

Preprints are preliminary reports that have not undergone peer review.
They should not be considered conclusive, used to inform clinical practice,
or referenced by the media as validated information.

The Regulatory Role of Monochromatic LED Light Quality in β- Carotene Accumulation and Carbon Flow Allocation in Photosynthetic Pathways of Dunaliella salina

Jiale Gu
Hohai University
Yongfu Li
liyongfu@hhu.edu.cn
Hohai University
Tianze Zhao
Hohai University
Delong Li
Hohai University
Xingkai Che
Hohai University
Ruiqian Li
Ocean University of China

Research Article

Keywords: Dunaliella salina, Light quality, Carbon allocation, Electron transport chain, Biomass composition, Transcriptomics

Posted Date: November 9th, 2026

DOI: https://doi.org/10.21203/rs.3.rs-11466429/v1

License: This work is licensed under a Creative Commons Attribution 4.0 International License.
Read Full License

Additional Declarations: No competing interests reported.

The Regulatory Role of Monochromatic LED Light Quality in β-Carotene Accumulation and Carbon Flow Allocation in Photosynthetic Pathways of *Dunaliella salina*

Jiale Gu[1] · Yongfu Li[1,2] · Tianze Zhao[1] · Delong Li[1,2] · Xingkai Che[1,2] · Ruiqian Li[3]

1 Jiangsu Province Engineering Research Center for Marine Bio-resources Sustainable Utilization, Observation and Research Station of Air-Sea Interface of Ministry of Natural Resources, College of Oceanography, Hohai University, Nanjing 210024, China

2 Yajiang Clean Energy Research Institute, Hohai University, LinZhi, 860114 China

3 Ocean University of China, Qingdao, 266237, China

* Correspondence: Yongfu Li, E-mail: liyongfu@hhu.edu.cn; Address: #8 Fochengxi Road, Jiangning District, Nanjing 211100, China

Abstract

Dunaliella salina is a valuable source of natural metabolites, including lipids, proteins, glycerol, and carotenoids. However, the physiological mechanisms through which light quality regulates carbon allocation and biomass synthesis remain unclear. Here, a two-stage culture strategy was used to investigate the effects of white (WL), blue (BL), red (RL), and green light (GL) on algal growth, biochemical composition, photosynthetic performance, and the expression of key genes involved in biomass synthesis. BL promoted cell growth and the accumulation of photosynthetic pigments and proteins, yielding a maximum specific growth rate of 0.053 ± 0.002 d^{-1} and a protein content of 381.86 ± 8.16 mg g^{-1}. Chlorophyll and carotenoid concentrations under BL reached 5.535 and 2.185 mg L^{-1}, respectively, exceeding those under the other treatments. These responses may be associated with enhanced photosynthetic electron transport, carbon assimilation, photosynthetic and respiratory activity, and reactive oxygen species-scavenging capacity. In contrast, RL produced the highest starch content (6.51 ± 0.10 mg g^{-1}), while WL and RL resulted in higher total lipid contents of 297.07 ± 2.59 and 288.98 ± 8.76 mg g^{-1}, respectively. Overall, light quality differentially affected growth

and biochemical accumulation in *D. salina*. The increased starch and lipid accumulation under RL and WL may reflect oxidative-stress-associated adjustments in carbon allocation and adaptive cellular responses.

Keywords *Dunaliella salina* · Light quality · Carbon allocation · Electron transport chain · Biomass composition · Transcriptomics

Introduction

Due to their rapid growth rate, high photosynthetic efficiency, and good environmental tolerance (Saini et al. 2020), microalgae have become an ideal source of various natural metabolites, such as proteins (Thangsiri et al. 2024; Yu et al. 2024), lipids (Zhang et al. 2022; Xue et al. 2016), polysaccharides (Kumar et al. 2024; Debnath et al. 2024), and carotenoids (Mu et al. 2016; Lamers et al. 2008). As a unicellular eukaryote belonging to the Chlorophyceae family, *Dunaliella salina* is capable of producing and storing various bioactive metabolites, such as lipids, proteins, glycerol, and carotenoids, within its cellular factories (Borowitzka 2013; Singh et al. 2023; Pais et al. 2024; Araj-Shirvani et al. 2024; Cheni et al. 2024). Reports indicate that *D. salina* cells can store up to 10% of their dry weight as carotenoids under photosynthetic autotrophic conditions (Ben-Amotz et al. 1982; Lam and Lee 2014). Till now, large-scale cultivation of *D. salina* has been primarily conducted in outdoor open ponds, carried out in countries such as Australia, Israel, and China (Del Campo et al. 2007; Borowitzka 2013; Li et al. 2020).

The two-stage culture strategy (TSCS) is a method designed to cultivate microalgae under optimized conditions to achieve high biomass, followed by maintaining biomass under stress conditions to enhance biomass content (Aziz et al. 2020; Jin et al. 2024). In TSCS-based *D. salina* cultivation, the objective of the first stage is to cultivate *D. salina* in an environment conducive to rapid cell growth to enhance biomass accumulation, which is referred to as the green cell phase of *D. salina*; the second stage focuses on transferring the microalgae cells to stress conditions—such as high light intensity, high temperature, and nitrogen deprivation—to increase biomass yield and productivity, which is referred to as the yellow cell phase of the microalgae.

To date, the two-stage culture method has been industrially applied to cultivate microalgae cells for carotenoid production (Ben-Amotz, 1995; Borowitzka and Borowitzka 1989; Borowitzka 2013). In both phases of the TSCS, photobioreactors play a positive role in carotenoid production (Prieto et al. 2011).

In large-scale microalgal cultivation using photobioreactors, light is a key factor influencing microalgal biomass and biomass accumulation. Among the various light parameters, light intensity and light quality are particularly critical, as they regulate microalgal growth and biomass synthesis (Chin et al. 2023; Li et al. 2026). Excessive light intensity can lead to photooxidation and photoinhibition in microalgae, while insufficient light intensity fails to support normal photosynthetic activity, thereby hindering microalgal growth (Esteves et al. 2024). Furthermore, specific light quality plays a regulatory role in microalgal cell growth and biomass synthesis. Changes in light quality prompt microalgal cells to adjust their metabolic patterns in response to environmental changes, thereby influencing microalgal growth and intracellular compound composition (Kim et al. 2014; Ueno et al. 2019). Under different light quality conditions, both enzyme activity and cellular chemical composition in microalgae undergo changes. Due to differences in photoreceptors among various microalgal species, the optimal light wavelengths also vary (Chen et al. 2023). It has been reported that microalgal cells divide more rapidly under red light, while those exposed to blue light exhibit larger cell sizes (Oldenhof et al. 2006; Li et al. 2021; Izadpanah et al. 2018; Wagner et al. 2016; Kim et al. 2014). However, numerous studies indicate that the effects of light quality on microalgal growth vary among species (Bialevich et al. 2022; McGee et al. 2020; Gatamaneni Loganathan et al. 2020).

In recent years, researchers have cultured *D. salina* cells under various light quality conditions to investigate the effects on cell growth and biomass accumulation. For example, Lan et al. (2022) used red light to enhance the expression of the LCYB gene in green *D. salina* cells to increase β-carotene content; Mirzaie et al. (2021) designed a red-blue flashing light switching system based on the growth curves of *D. salina* cells to enhance β-carotene synthesis within the cells; Sui et al. (2021) investigated the effects of different light qualities (red, blue, and white light) on β-

carotene production in two *Dunaliella* species and reported that red light increased the 9-cis/all-trans-β-carotene ratio; Mohebi Najafabadi and Naeimpoor (2023) applied red, blue, or mixed monochromatic light to *D. salina* cells during the two stages of a two-phase culture system to investigate the effects on intracellular β-carotene content; Mohanta et al. (2024) optimized light conditions (light intensity and quality) to enhance lipid accumulation in *D. salina* cells. However, to date, few studies have investigated the effects of monochromatic light on cellular energy allocation, carbon flux distribution, and the expression of related genes in *D. salina*. The regulatory mechanisms by which light quality influences primary metabolic processes, particularly photosynthesis and respiration, remain poorly understood.

In this study, the effects of different light qualities on energy metabolism and carbon allocation in *D. salina* were investigated through physiological and biochemical measurements, including cell density, cell dry weight, pigment content, respiratory oxygen consumption rate, photosynthetic oxygen evolution rate, chlorophyll fluorescence parameters, reactive oxygen species (ROS) levels, antioxidant enzyme activities, and intracellular biochemical composition, combined with whole-transcriptome sequencing. Furthermore, the expression levels of key genes involved in photosynthesis and respiration under different light conditions were analyzed to gain insights into the regulatory mechanisms of these primary metabolic processes and to provide a scientific basis for optimizing the two-stage cultivation strategy of *D. salina*.

Materials and Methods

Algal Strain and Culture Methods

Dunaliella salina (IOCAS 879ss) was obtained from the Institute of Oceanology, Chinese Academy of Sciences (Qin et al. 2021). The algal cells were cultured through a modified Johnson's medium (Borowitzka 1988). All *D. salina* cultures were maintained at 30 ± 1°C, under an irradiance of 80 ± 10 μmol m^{-2} s^{-1} (provided by white light-emitting diodes (LEDs)), and a 12-h light/12-h dark cycle until they reached the exponential growth phase. To prevent cell adhesion, the conical flasks containing the

cultures were manually shaken three times daily.

Algal Strain and Culture Methods

To investigate the effects of different light qualities, the experiment was conducted in a precision multi-light-quality combination tunable light incubator (Taizhou Haijiang Bioengineering Technology Co., Ltd., China), with a controlled cultivation temperature of 30 ± 1°C and a light-dark cycle of 12 h:12 h. Lighting was provided by four artificial light sources in different spectral regions: blue LED strips, red LED strips, white LED strips, and green LED strips. To ensure spectral purity, opaque steel plates were used to isolate the different spectral zones. A spectral flicker photometer (OHSP-350SF, Hangzhou Hongpu Optical Technology Co., Ltd., China) was used to measure the spectra of the artificial light sources in different light quality zones within the light-controlled incubator between 350 and 700 nm with a resolution of 1 nm (Fig. 1). Three biological replicates were set up for each light quality condition. *D. salina* cells were cultured for a total of 50 days, and the light management strategies during the culture period are shown in Table 1.

Table 1 Light Management during Culturing

Experimental period (d)	Light intensity (μmol m^{-2} s^{-1})
0~5	50±5 (LL)
5~30	100±10 (ML)
30~50	200±20 (HL)

To simulate the physiological transition from vegetative growth to stress-induced metabolism during the two-stage cultivation of *D. salina*, a three-stage strategy with progressively increasing light intensity was applied over a 50-day cultivation period. Light intensities were maintained at 50 ± 5, 100 ± 10, and 200 ± 20 μmol m^{-2} s^{-1} during days 0-5, 5-30, and 30-50, respectively. This strategy was designed according to the stage-specific light requirements and tolerance of *D. salina* to sequentially facilitate cellular acclimation, biomass accumulation, and stress induction. The gradual increase in irradiance was intended to minimize premature photoinhibition associated with

excessive light exposure during the early growth phase while providing sufficient light to support biomass production and subsequent stress-induced metabolic responses. Such temporal separation of the growth and induction phases may help balance the physiological trade-off between cell proliferation and the accumulation of stress-responsive metabolites, particularly β-carotene (Xi et al. 2021; Kim et al. 2024a, b).

During the initial cultivation phase (days 0–5), low-light (LL) conditions were employed primarily to facilitate the adaptation of newly inoculated cells to the culture environment and to reduce the risks associated with excessive excitation of the photosynthetic apparatus, reactive oxygen species (ROS) accumulation, and PSII photoinhibition caused by a sudden increase in light intensity. Recent studies have shown that low-light conditions can maintain relatively stable photochemical activity and photosynthetic electron transport in *D. salina*, whereas high-light exposure can rapidly decrease PSII activity and induce pronounced oxidative stress responses (Kim et al. 2024b; Zhao et al. 2025). Accordingly, a relatively low light intensity was applied during the initial cultivation stage to minimize the risk of photoinhibition while maintaining sufficient light for basal photosynthetic activity, thereby facilitating acclimation of the photosynthetic apparatus and providing a stable physiological basis for subsequent cell growth.

Once the cells had completed their initial acclimation, the light intensity was increased to 100 ± 10 μmol m^{-2} s^{-1} (ML) during days 5–30 to enhance photosynthetic carbon fixation and cell proliferation, thereby promoting biomass accumulation and establishing a sufficiently high cell density for the subsequent induction stage. This phase corresponded to the vegetative growth stage of the conventional two-stage cultivation strategy, in which the primary objective was to sustain efficient photosynthetic activity while avoiding premature exposure to excessive light stress. Previous studies have shown that the growth and β-carotene accumulation of *D. salina* depend strongly on the amount of light received by individual cells; appropriate irradiance supports biomass production, whereas excessive irradiance can progressively redirect cellular metabolism from growth toward photoprotective responses (Xi et al. 2021). Accordingly, moderate light intensity was maintained during

days 5–30 to balance light-energy supply and the risk of photoinhibition, thereby favoring the allocation of photosynthetically fixed carbon toward cell proliferation and biomass accumulation and providing an adequate cellular basis for the subsequent stress-induction stage.

From days 30 to 50, the light intensity was further increased to 200 ± 20 μmol m^{-2} s^{-1} (HL). As cell density increases, light absorption and scattering within the culture become more pronounced, resulting in stronger self-shading and a reduction in the effective photon supply to individual cells. Increasing the incident irradiance can therefore partially compensate for light attenuation in dense cultures (Xi et al. 2021). In addition, enhanced irradiance increases excitation pressure on the photosynthetic apparatus and promotes ROS-mediated signaling, which can activate carotenoid biosynthetic pathways and stimulate the accumulation of photoprotective metabolites, particularly β-carotene (Chen et al. 2024; Kim et al. 2024a, b). Previous studies have shown that, under high-light conditions, cellular metabolism in *D. salina* can shift from rapid growth toward carotenoid biosynthesis and photoprotective responses, whereas prolonged exposure to excessive irradiance may suppress cell growth. Accordingly, high-light treatment was initiated only after sufficient biomass had accumulated, thereby separating the biomass accumulation and stress induction phases and mitigating the trade-off between cell growth and stress-responsive metabolism.

In summary, this study employed a stepwise increase in light intensity (50 → 100 → 200 μmol m^{-2} s^{-1}) and introduced an initial low-light acclimation phase into the conventional two-stage cultivation strategy of biomass accumulation followed by stress induction, thereby establishing a three-stage cultivation strategy comprising low-light acclimation, moderate-light growth, and high-light induction. This strategy can alleviate light stress during the early cultivation phase and enables higher biomass accumulation during the middle phase; in the late cultivation phase, it can promote the synthesis of photoprotective metabolites such as β-carotene by compensating for light attenuation within the system and applying strong light stress.

Algal cells were harvested every 5 days for cell imaging, cell density, and photosynthetic pigment measurements. On day 50, all *D. salina* cells were harvested

for the determination of intracellular physiological and biochemical parameters, photosynthetic and respiratory rates, reactive oxygen species (ROS) levels, and antioxidant enzyme activity, as well as for transcriptomic analysis.

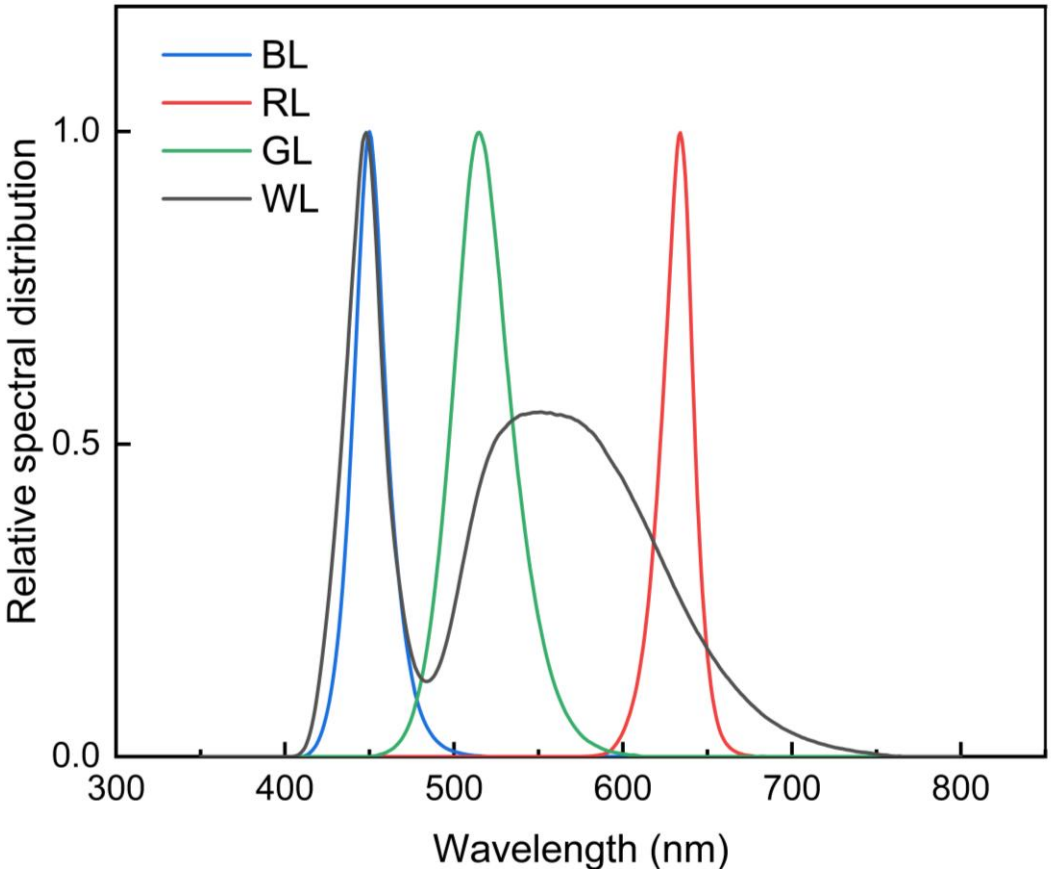


Fig. 1 Relative Emission Spectra of Artificial Light Sources Applied in Photobioreactors

Determination of Cell Morphology, Dry Weight, Algal Cell Density, and Specific Growth Rate

Recording of algal cell and algal culture images: Changes in the color of the algal culture in the cell culture flask were observed with the naked eye and photographs were taken for documentation. Algal cell density was determined by manual counting using a hemocytometer and a 37 XB inverted microscope (Shanghai Optical Instrument Factory, Co., Ltd., China).

Determination of *D. salina* dry weight: The ash-free dry weight (AFDW) of *D. salina* biomass was determined using the gravimetric method (Sui et al. 2021). First, a clean glass weighing dish was placed on an analytical balance (CP114, Ohaus

Instruments (Changzhou) Co., Ltd., China) and weighed, with the weight recorded as M1. Next, 60 mL of algal suspension is centrifuged at 8,000 g for 10 minutes; the supernatant was discarded, and all the precipitate was collected into the glass weighing dish. The glass weighing dish was then placed in a 105°C oven and dried for 48 h. Afterward, the glass weighing dish was transferred to a desiccator. Once cooled to room temperature, it was placed on an analytical balance (CP114, Ohaus Instruments (Changzhou) Co., Ltd., China) and weighed, with the weight recorded as M2. AFDW is calculated using the following formula:

$$\mathrm{AFDW}\ (g/L) = \frac{M_1 - M_2}{V}$$

Here, M1 and M2 (mg) are the recorded weights, and V is the volume of the centrifuged microalgal suspension (60 mL).

Determination of algal cell density and specific growth rate: Algal cell density was determined by manual counting using a hemocytometer and a 37XB inverted microscope (Shanghai Optical Instrument Factory, Co., Ltd., China). The specific growth rate (μ) of *D. salina* cells was calculated using the following formula (Moheimani and Parlevliet 2013):

$$\mu = (\ln N_2 - \ln N_1)/(T_2 - T_1)$$

In this context, N2 (final) and N1 (initial) respectively represent the cell densities (cells/mL) measured using a hemocytometer at times T2 and T1.

Determination of Pigment Content

Determination of chlorophyll *a* and *b* (Chl *a* and Chl *b*): The concentrations of Chl *a* and Chl *b* in the cultures were determined using a modified ethanol extraction method based on Danesh et al. (2017) and the spectrophotometric method described by Arnon (1949). Briefly, 2 mL of algal suspension was centrifuged at 8,000 × *g* for 10 min, and the resulting cell pellet was subjected to lysis in a boiling water bath for 2 min. Subsequently, 2 mL of 96% ethanol was added to the lysed cells, and the mixture was thoroughly mixed and heated in a boiling water bath for 15 min. The mixture was then centrifuged at 8,000 × *g* for 10 min to separate the pigment-containing supernatant. The

absorbance of the supernatant was measured at 665, 649, and 470 nm (A_{665}, A_{649}, and A_{470}, respectively) using a spectrophotometer (756S, Shanghai Guangling Technology Co., Ltd., China). The concentrations of chlorophyll *a* and chlorophyll *b* (mg L^{-1}) were subsequently calculated according to the corresponding equations.

Determination of β-carotene: The β-carotene content was determined using high-performance liquid chromatography (HPLC) according to the method described by Priscilla et al. (2024). Briefly, 2 mL of algal suspension was centrifuged at 8,000 × *g* for 10 min, and the resulting cell pellet was subjected to lysis in a boiling water bath for 2 min. Subsequently, 2 mL of 96% ethanol was added to the lysed cells, and the mixture was thoroughly mixed and heated in a boiling water bath for 15 min. The mixture was then centrifuged at 8,000 × *g* for 10 min to obtain the pigment-containing supernatant. An aliquot of 20 μL of the pigment extract was transferred to an HPLC vial and injected into the HPLC system for analysis.

The chromatographic analysis was performed using an Agilent 1260 Infinity II HPLC system equipped with a C30 YMC™ Carotenoid column (4.6 mm × 250 mm, 5 μm). The mobile phase consisted of solvent A [acetonitrile/methanol (3:1, v/v) containing 0.05% triethylamine (v/v)] and solvent B [methyl tert-butyl ether (MTBE) containing 0.05% triethylamine (v/v)]. Both mobile phases were degassed by ultrasonication prior to use. The gradient elution program was as follows: the proportion of mobile phase B was linearly increased from 0% to 55% over 8 min and then maintained at 55% for 27 min. The flow rate was set at 1.0 mL min^{-1}, the detection wavelength was 475 nm, the injection volume was 20 μL, and the column temperature was maintained at 30 °C.

Determination of Chlorophyll Fluorescence Parameters

Following the method described by Li et al. (2024), Chl *a* fluorescence transients were measured using a FluorPen chlorophyll fluorometer (AquaPen-Ap110-C, Czech Republic). Prior to measurement, algal suspensions from different light quality treatments were transferred to cuvettes and dark-adapted for 20 min. Nine parallel technical measurements were performed for each treatment. Saturated red light at 3000

μmol m^{-2} s^{-1} was generated by a light-emitting diode (LED) array with a peak wavelength of 650 nm. Chl *a* fluorescence transient parameters were obtained using a 2-s saturating red-light pulse, and the OJIP transients were analyzed according to the OJIP test protocol proposed by Strasser (1995). The relevant Chl *a* fluorescence transient parameters and their biological significance are presented in Table 2.

Table 2 Chl *a* Fluorescence Transient Parameters (Strasser *et al*. 2004)

Parameters	Biological significance
Fv/Fm	Maximum photochemical efficiency of the PSII
PI_{ABS}	Performance index on absorption basis
ABS/RC	Absorption flux per RC
TR_0/RC	Trapped energy flux per RC (at t=0)
ET_0/RC	Electron transport flux per RC (at t=0)
DI_0/RC	Dissipated energy flux per RC (at t=0)
1-Vj	Probability (at t = 0) that a trapped exciton moves an electron into the electron transportchain beyond Q_A^-

Determination of Photosynthetic Oxygen Evolution Rate and Respiration Rate

Following the method described by Li et al. (2024), an oxygen electrode (YQZ-201A, Yizongqi Technology Co., Ltd., Beijing) was used. Net photosynthetic oxygen evolution rate and respiratory oxygen uptake rate were measured at 20 ± 1 °C. Approximately 14 mL of algal suspension was placed in the electrode chamber, and 1 mL of saturated $KHCO_3$ solution was added to generate sufficient CO_2 for photosynthetic reactions. The electrode chamber was then sealed with the electrode. Oxygen release was subsequently measured under a photosynthetic light intensity of 200 μmol m^{-2} s^{-1}. Dark respiration was estimated based on oxygen uptake by algal cells in the dark. The true photosynthetic rate was calculated as the sum of the oxygen release rate and the dark respiration rate.

Determination of Reactive Oxygen Species (ROS) and Antioxidant Enzyme Activity

Reactive oxygen species (ROS) levels and oxidative damage in *D. salina* cells were characterized by measuring the concentrations of hydrogen peroxide (H_2O_2) and malondialdehyde (MDA), respectively (Bamary et al. 2022). Antioxidant enzyme activity was primarily assessed by measuring the activities of superoxide dismutase (SOD) and ascorbate peroxidase (APX) (Singh et al. 2023).

After 50 days of cultivation under different light conditions, the concentrations of malondialdehyde (MDA) and hydrogen peroxide (H_2O_2) in *D. salina* cells, as well as the activities of superoxide dismutase (SOD) and ascorbate peroxidase (APX), were determined. A 50 mL aliquot of algal suspension was centrifuged at 10,000 × *g* and 4 °C for 10 min to collect the cell pellet. The collected cell pellet was ground in a mortar and pestle with pre-chilled extraction buffer (50 mM phosphate buffer, pH 7.8) in the presence of liquid nitrogen.

The H_2O_2 content was determined according to the method proposed by Ferguson et al. (1983). Following centrifugation at 10,000 × *g* for 10 min, 0.6 mL of 20% titanium tetrachloride ($TiCl_4$) and 0.4 mL of 30% ammonium hydroxide were added to 1 mL of the supernatant. The mixture was then centrifuged at 4,000 × *g* for 15 min. Subsequently, 20% (v/v) sulfuric acid (H_2SO_4) was added to the resulting precipitate to dissolve it. The absorbance was measured at 410 nm.

The MDA content was determined according to the method proposed by Heath and Packer (1968). Following centrifugation at 10,000 × *g* for 10 min, 2 mL of 0.6% (v/v) thiobarbituric acid (TBA) was added to 2 mL of the supernatant. The mixture was incubated in a 100 °C water bath for 15 min, cooled, and then centrifuged at 3,000 × *g* for 10 min. The absorbance of the supernatant was measured at 450, 530, and 600 nm.

The activities of SOD and APX were determined using a Superoxide Dismutase Assay Kit and an Ascorbate Peroxidase Assay Kit, respectively (Nanjing Jiancheng Institute of Biological Engineering). SOD catalyzes the dismutation of O_2^- to O_2 and H_2O_2, whereas APX is a peroxidase that uses ascorbate as an electron donor and plays a key role in H_2O_2 scavenging in chloroplasts. The activities of SOD and APX can serve as indirect indicators of oxidative stress in *D. salina* (Li et al. 2024; Guermazi et al. 2023).

Determination of Intracellular Protein, Total Fat, Glycerol, and Starch Content

The determination of protein content followed the method proposed by Araj-Shirvani et al. (2024). Polyvinylpyrrolidone (0.05 g) and phosphate buffer (pH 7) were mixed with 100 mL of *D. salina* cell suspension, followed by centrifugation at 9000 g for 3 minutes. The supernatant was mixed with 2 mL of Coomassie Brilliant Blue dye, and the absorbance of the mixture at 595 nm was measured using a UV-visible spectrophotometer (756S, Shanghai Lengguang Technology Co., Ltd., China). Protein content was calculated based on a standard curve prepared using bovine serum albumin (Bradford 1976).

The determination of starch content was based on the method proposed by Mirshekari et al. (2019). The algal cell pellet (obtained by centrifuging 60 mL of algal suspension at 10,000 g for 10 minutes) was decolorized with acetone and extracted with 80% (v/v) ethanol to remove all soluble sugars. Subsequently, starch was extracted from the sugar-free cell pellet using a modified acid hydrolysis method (Mirshekari et al. 2019). Finally, the starch content was calculated by measuring the glucose concentration in the extract using the anthrone-sulfuric acid method.

The glycerol content was determined according to the method proposed by Chen et al. (2019). The algal cell pellet, obtained by centrifuging 30 mL of algal suspension at 10,000 × *g* for 10 min, was extracted with 1.5 mL of distilled water and 0.2 mL of chloroform. The mixture was subjected to ultrasonic disruption twice for 30 s each, with a 2-min interval between the two treatments, followed by centrifugation at 12,000 × *g* for 10 min. Subsequently, 0.2 mL of the glycerol-containing supernatant was mixed with 1 mL of sodium periodate reagent, consisting of 3 mM sodium periodate and 100 mM ammonium acetate dissolved in 100 mL of 6% acetic acid. After 5 min, 2.5 mL of acetone–isopropanol reagent (acetone/isopropanol, 1:99, v/v) was added to the mixture. The mixture was then incubated in a 60 °C water bath for 30 min, and its absorbance at 410 nm was measured using a UV–Vis spectrophotometer. The glycerol concentration was calculated based on a glycerol calibration curve.

The determination of total lipid content was based on the method proposed by

Bligh and Dyer (1959). Total lipid content was determined using the chloroform-methanol method followed by gravimetric analysis. The algal pellet (obtained by centrifuging 60 mL of algal suspension at 10,000 g for 10 minutes) was weighed on an analytical balance and extracted with a chloroform: methanol (2:1, v/v) solution. The mixed solution was centrifuged at 10,000 g for 10 minutes to separate the organic phase from the aqueous phase. The organic phase was transferred to a pre-weighed weighing flask and placed in a constant-temperature forced-air drying oven (DGG-9240A, Shanghai Senxin Laboratory Instrument Co., Ltd., China) at 120°C until it reached a constant weight. The weighing flask was then weighed on an analytical balance after evaporation and drying, and the total lipid content was calculated accordingly.

Transcriptomic Analysis

RNA sequencing and standard bioinformatics analysis were performed by Shanghai Majorbio Bio-pharm Biotechnology Co., Ltd. (Shanghai, China) (Liu et al. 2023). In brief, total RNA was extracted from BL, RL, WL, and GL-treated samples, and first-strand cDNA was synthesized using random hexamer primers and M-MuLV reverse transcriptase. To select cDNA fragments with a preferred length of 240 bp, library fragments were purified using the AMPure XP system (Beckman Coulter). Next, 3 μL of USER enzyme (NEB) was incubated with the size-selected, adapter-ligated cDNA for 15 minutes at 37°C, followed by 5 minutes at 95°C, prior to PCR. PCR was then performed using Adhesion high-fidelity DNA polymerase, universal PCR primers, and Index (X) primers. Finally, the PCR products were purified (AMPure XP system) and library quality was assessed on an Agilent Bioanalyzer 2100 system. The library was then sequenced using the Illumina HiSeq X-ten platform with 240 bp paired-end (PE) reads. Use the BMKCloud (www.biocloud.net) online bioinformatics pipeline. Annotate gene functions based on the following databases: NR (NCBI Non-Redundant Protein Sequences), Pfam (Protein Families), KOG/COG/eggNOG (clusters of protein orthologous groups), Swiss-Prot (a manually annotated and reviewed protein sequence database), KEGG (Kyoto Encyclopedia of Genes and Genomes), and GO (Gene Ontology), with a threshold of $|\log2FC| > 1$ and a false discovery rate (FDR) < 0.05.

Three biological replicates were analyzed for each light treatment. GO and KEGG pathway enrichment analyses were conducted using the Kolmogorov-Smirnov test based on the topGO R package and the KOBAS software, respectively. The raw read-sequencing data have been deposited in the NCBI database under accession number PRJNA1165417.

Statistical Analysis

Data in the Fig.s are presented as "mean ± standard deviation (SD)" for replicates. One-way analysis of variance (ANOVA) was performed, supplemented by LSD post-hoc tests. All analyses were conducted using SPSS Statistics 26.0 software. All data were subjected to normality and homogeneity of variance tests to confirm their suitability for statistical analysis. When significant differences were detected, post-hoc comparisons of means (Tukey or Games-Howell tests) were performed to identify which values differed significantly. A p-value less than 0.05 was considered statistically significant.

Results

Effects of Monochromatic Light Quality on *Dunaliella* Cells

HL irradiation caused rapid morphological changes in *D. salina* cells. After switching from medium light (ML, 100 ± 10 μmol m^{-2} s^{-1}) to high light (HL, 200 ± 20 μmol m^{-2} s^{-1}), Cell morphology and growth patterns were examined. Both the *D. salina* culture and cells under BL, RL, and WL began to turn orange, whereas those under GL remained green (Fig. 2A, B). This indicates that upon the transition from ML to HL, carotenoids rapidly accumulated in *D. salina* cells under BL, RL, and WL, whereas *D. salina* cells under GL did not accumulate carotenoids in significant amounts.

During the 50-day cultivation cycle, the highest cell density and dry weight were observed in *D. salina* under BL treatment (Fig. 3A, B). During the 0–5-day low-light (LL, 50 ± 5 μmol m^{-2} s^{-1}) acclimation period, the specific growth rates under RL and WL were significantly higher than those under BL and GL, indicating that *D. salina* under RL and WL could adapt to the new environment more quickly than those under BL and GL. During the medium-light (ML, 100 ± 10 μmol m^{-2} s^{-1}) growth phase from

406 days 5 to 30, the highest specific growth rate (μ) was observed under BL exposure
407 (0.0129 ± 0.0003 d^{-1}), slightly higher than the specific growth rates under WL (0.0078
408 ± 0.0023 d^{-1}) and GL (0.0037 ± 0.0026 d^{-1}), and significantly higher than that under RL
409 (0.0025 ± 0.0017 d^{-1}). This indicates that *D. salina* under BL exposure grows better
410 than under other light conditions in a suitable environment. During the 30–50-day
411 period of high-light (HL, 200 ± 20 μmol m^{-2} s^{-1}) stress, the growth rates of *D. salina*
412 under all light conditions were inhibited to varying degrees. The μ values for algal cells
413 exposed to WL and RL were -0.01 ± 0.0002 d^{-1} and -0.003 ± 0.0018 d^{-1}, respectively,
414 whereas algal cells exposed to BL and GL light still maintained a certain degree of
415 growth, with μ values of 0.002 ± 0.0023 d^{-1} and 0.003 ± 0.0007 d^{-1}, respectively. This
416 indicates that *D. salina* exposed to BL and GL light adapted better to the stress
417 environment than those exposed to WL and RL. Throughout the entire 50-day
418 cultivation period, the specific growth rate of *D. salina* under BL exposure (0.053 ±
419 0.002 d^{-1}) was significantly higher than that under other light conditions (0.046 ± 0.002
420 d^{-1}; 0.043 ± 0.002 d^{-1}; 0.045 ± 0.001 d^{-1}), indicating that BL exposure was more
421 conducive to cell division and proliferation in *D. salina* than other light conditions
422 throughout the entire cultivation period (50 days) (Fig. 3C).

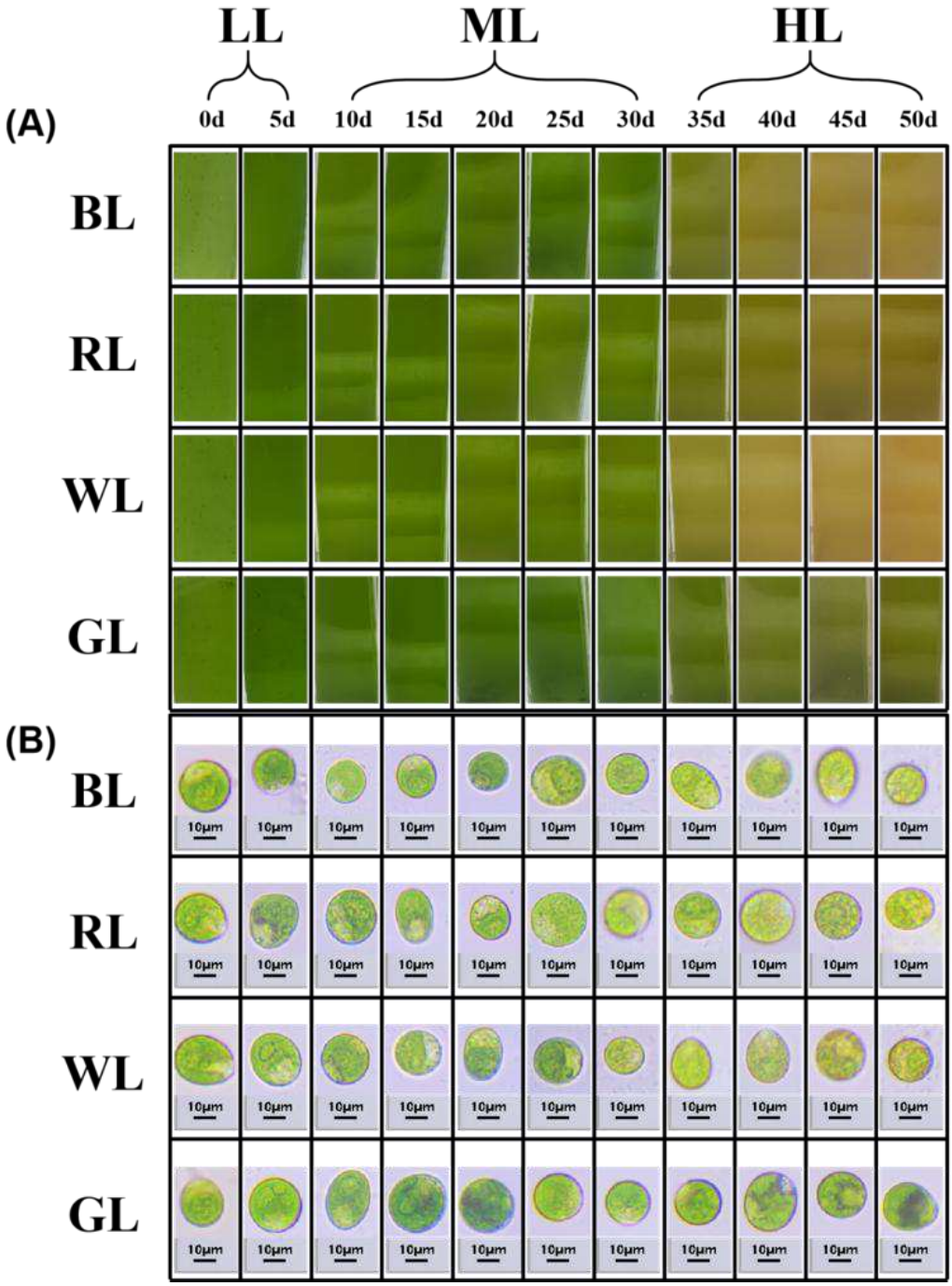


Fig. 2 Changes in the color of the algal culture (**A**) and cell morphology (**B**) of *Dunaliella salina* after 50 days of cultivation under gradient illumination with blue light (BL), red light (RL), green light (GL), and white light (WL)

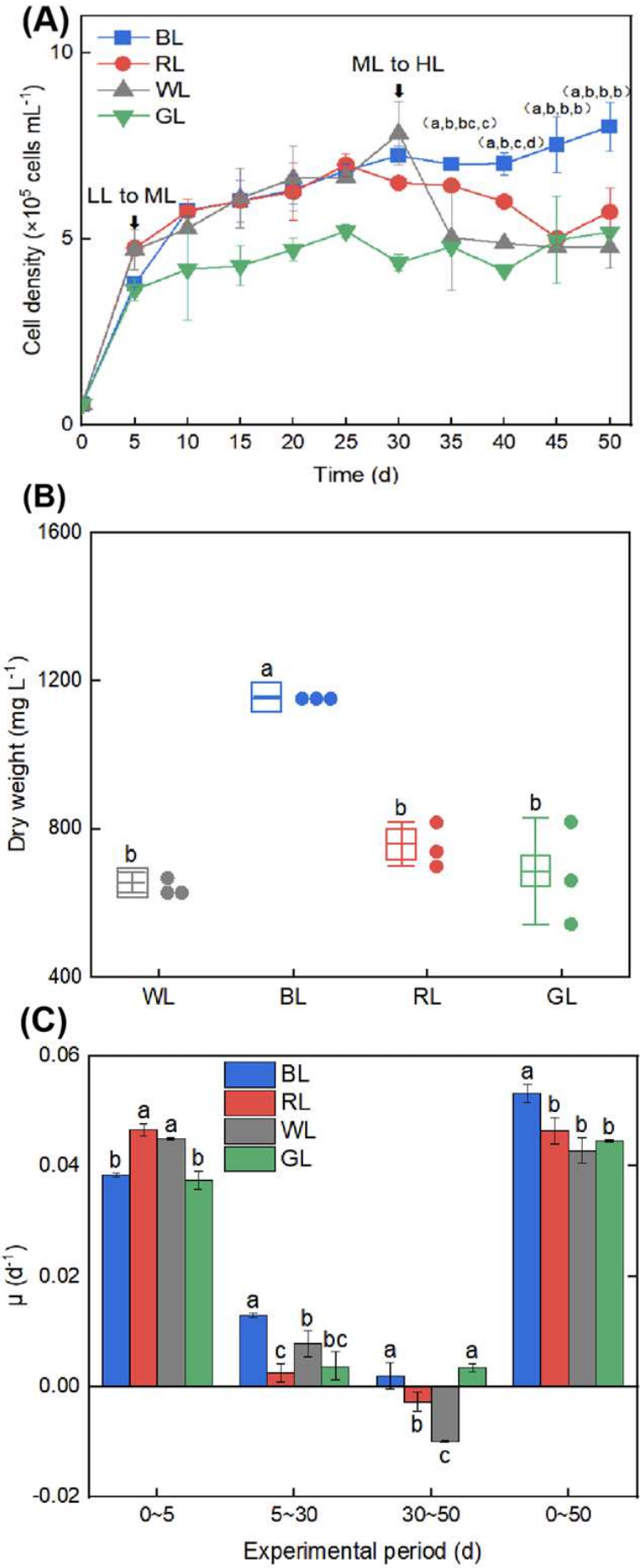
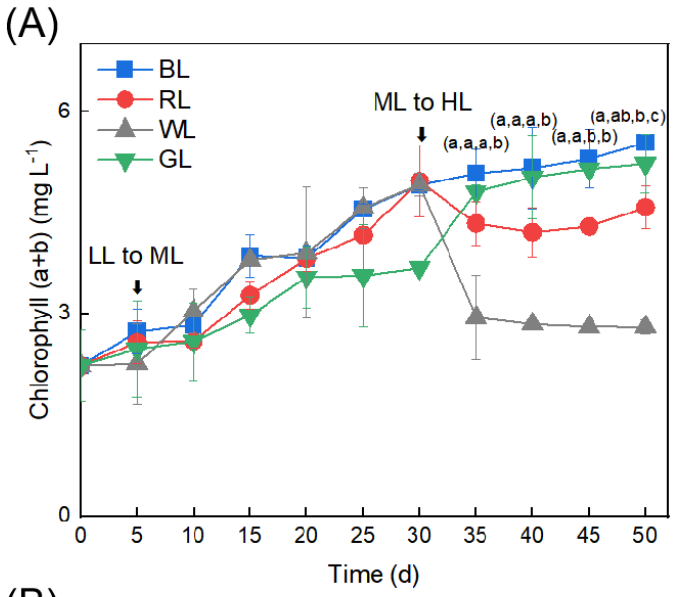
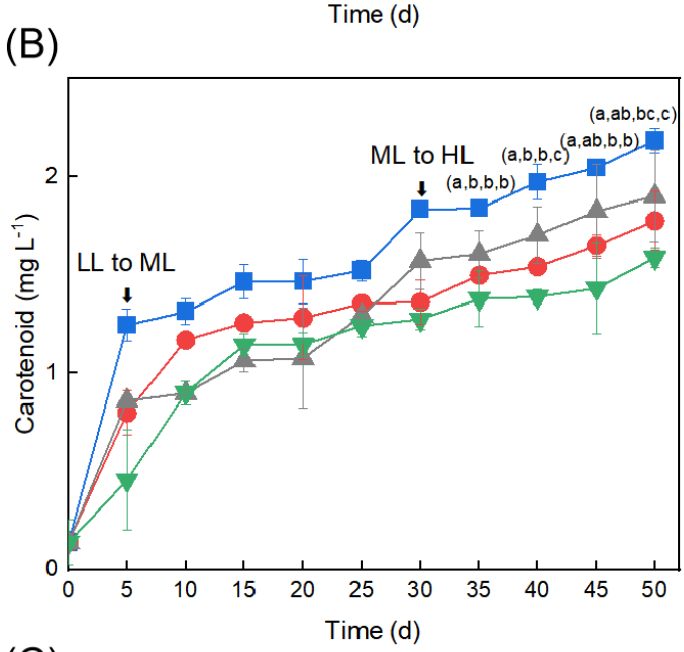

(A)
BL
RL
WL
GL
ML to HL
LL to ML
(a,b,b,b)
(a,b,b,b)
(a,b,bc,c)
(a,b,c,d)
Cell density (×10^5 cells mL^-1)
Time (d)
(B)
Dry weight (mg L^-1)
WL
BL
RL
GL
(C)
μ (d^-1)
0~5
5~30
30~50
0~50
Experimental period (d)

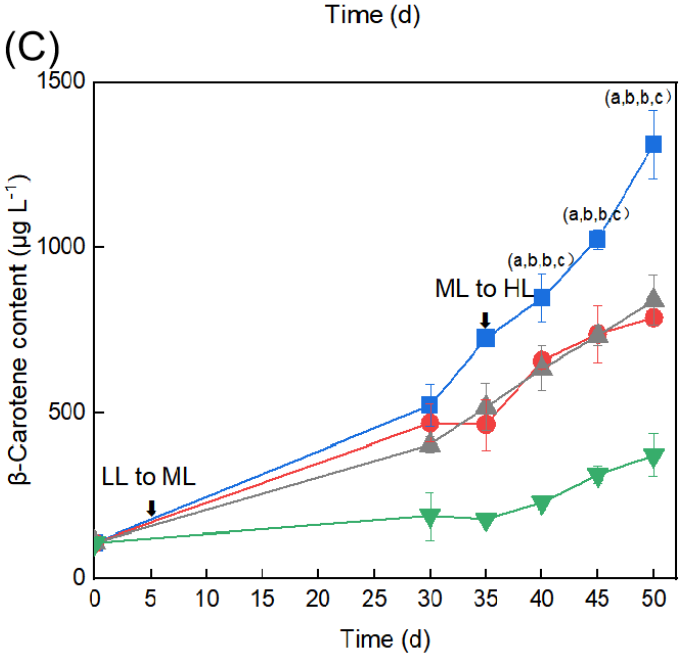
Fig. 3 Growth curves (**A**), dry weight (**B**), and specific growth rates (**C**) of halophilic *Dunaliella* after 50 days of cultivation under blue light (BL), red light (RL), green light (GL), and white light (WL) gradients. Data represent the mean ± SD of three biological replicates. Different letters (e.g., a, b, and c) between treatment groups indicate significant differences ($P < 0.05$)

Effect of Light Quality on Pigment Content in *Dunaliella*

Since the chlorophyll in *D. salina* consists of chlorophyll *a* and chlorophyll *b*, the total chlorophyll content is expressed as chlorophyll (*a*+*b*) (Araj-Shirvani et al. 2024). During the 50-day cultivation period, *D. salina* exposed to BL and GL had higher chlorophyll content than those under RL and WL. Notably, during the medium-light (ML, 100 ± 10 μmol m^{-2} s^{-1}) growth phase from days 5 to 30, there were no significant differences in chlorophyll content among the BL, RL, and WL treatments ($P > 0.05$), but they were significantly higher than in the GL treatment. However, after transition from medium light (ML, 100 ± 10 μmol m^{-2} s^{-1}) to high light (HL, 200 ± 20 μmol m^{-2} s^{-1}), the chlorophyll content in the RL and WL treatments decreased significantly, the growth rate of chlorophyll content in *D. salina* under the BL treatment slowed, whereas chlorophyll content in *D. salina* under the GL treatment increased significantly; this may be related to the fact that *D. salina* under GL was still in the green cell stage (Fig. 4A). The carotenoid and β-carotene contents of *D. salina* exposed to BL were significantly higher than those under other light conditions throughout the 50-day cultivation period (Fig. 4B, C). In summary, over the 50-day cultivation period, *D. salina* exposed to BL exhibited the highest chlorophyll, carotenoid, and β-carotene contents, indicating that BL exposure is more conducive to the synthesis of chlorophyll, carotenoids, and β-carotene in *D. salina* cells.


(A)
BL
RL
WL
GL
ML to HL
LL to ML
(a,a,a,b)
(a,a,a,b)
(a,a,b,b)
(a,ab,b,c)
Chlorophyll (a+b) (mg L-1)
Time (d)
0
3
6
0
5
10
15
20
25
30
35
40
45
50


(B)
ML to HL
LL to ML
(a,b,b,b)
(a,b,b,c)
(a,ab,b,b)
(a,ab,bc,c)
Carotenoid (mg L-1)
Time (d)
0
1
2
0
5
10
15
20
25
30
35
40
45
50


(C)
ML to HL
LL to ML
(a,b,b,c)
(a,b,b,c)
(a,b,b,c)
β-Carotene content (μg L-1)
Time (d)
0
500
1000
1500
0
5
10
15
20
25
30
35
40
45
50

451

Fig. 4 Chlorophyll concentration (**A**), carotenoid concentration (**B**), and β-carotene concentration (**C**) of halophilic *Dunaliella* after 50 days of cultivation under blue light (BL), red light (RL), green light (GL), and white light (WL) gradients. Data represent the mean ± SD of three biological replicates. Different letters (e.g., a, b, and c) among treatment groups indicate significant differences ($P < 0.05$)

Effects of Light Quality on the Cellular Composition of *Dunaliella*

After 50 days of cultivation, the protein, total lipid, glycerol, and starch contents of *D. salina* grown under different light quality conditions were determined (Fig. 5). The highest protein content was observed under blue light (BL) treatment (381.86 ± 8.16 mg g^{-1}), which was significantly higher than those under white light (WL; 297.54 ± 4.05 mg g^{-1}), red light (RL; 294.95 ± 6.17 mg g^{-1}), and green light (GL; 248.42 ± 9.81 mg g^{-1}). In contrast, the total lipid content was highest under WL (297.07 ± 2.59 mg g^{-1}), followed closely by RL (288.98 ± 8.76 mg g^{-1}), with significantly lower values observed under GL (268.13 ± 0.89 mg g^{-1}) and BL (226.10 ± 24.86 mg g^{-1}) compared with WL. Glycerol content was lowest under GL treatment (0.73 ± 0.26 mg g^{-1}), significantly lower than that under the other light conditions. Starch accumulation was most pronounced under RL, reaching 6.51 ± 0.10 mg g^{-1}, which was significantly higher than the values recorded under GL (5.15 ± 0.68 mg g^{-1}), BL (3.36 ± 0.18 mg g^{-1}), and WL (2.74 ± 0.01 mg g^{-1}). Collectively, these results indicate that light quality differentially influences the biochemical composition of *D. salina*. Specifically, BL favors protein accumulation, WL and RL are associated with relatively high lipid contents, GL appears to suppress glycerol accumulation, and RL promotes starch accumulation.

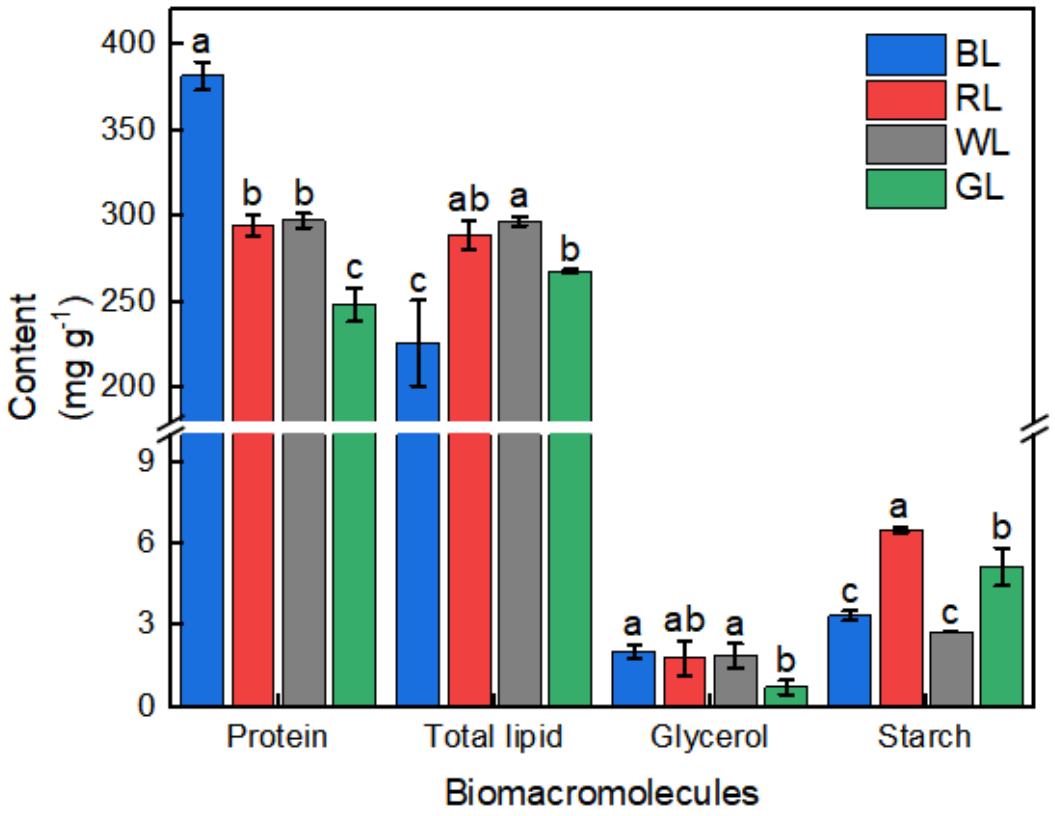


Fig. 5 Protein, total lipid, glycerol, and starch contents of *Dunaliella salina* cultured for 50 days under blue light (BL), red light (RL), green light (GL), and white light (WL) gradients. Data represent the mean ± SD of three biological replicates. Different letters (e.g., a, b, and c) between treatment groups indicate significant differences ($P < 0.05$)

Effects of Light Quality on the Photosynthesis of *Dunaliella salina*

After a 50-day cultivation period, the photosynthetic oxygen evolution rate, chlorophyll fluorescence parameters, and gene expression levels in the photosynthetic pathways (photosynthetic phosphorylation and the Calvin cycle) of *D. salina* were measured under different light quality conditions. The photosynthetic oxygen evolution rate of *D. salina* cells exposed to BL and GL was significantly higher than that of cells exposed to WL and RL (Fig. 6A). Analysis of chlorophyll fluorescence parameters revealed significant differences in the effects of different light qualities on the photosynthetic capacity of *D. salina* cells and the light energy absorption of the PSII reaction center (RC). Fv/Fm and Pi_ABS values measured under BL and GL were significantly higher than those under WL and RL, whereas DI_0/RC values were higher under WL and RL

compared to other light conditions. This indicates that more light energy was dissipated by *D. salina* under WL and RL, suggesting that *D. salina* exhibits higher photosynthetic capacity and reaction center photosynthetic efficiency under BL and GL. In contrast, the photosynthetic capacity and photosynthetic efficiency of the reaction centers in *D. salina* were significantly impaired under WL and RL, resulting in a substantial increase in the amount of light energy dissipated due to inability to utilize it (Fig. 6B).

As shown in Fig. 6C, differentially expressed genes (DEGs) were identified in the four complexes of the photosynthetic phosphorylation pathway (KO: 00195). Under different light conditions, two genes were differentially expressed in the PSII complex; two genes were differentially expressed in the cytochrome b6f (Cyt b6f) complex; and five genes were differentially expressed in the PSI complex; and six genes in the ATP synthase complex. Notably, these differentially expressed genes were upregulated under BL exposure compared to other light conditions. This suggests that BL is more conducive to electron transport in the photosynthetic phosphorylation pathway of *D. salina*. As shown in Fig. 6D, three enzyme genes in the Calvin cycle (KO:00710) were differentially expressed, namely fructose-1,6-bisphosphatase (FBP), glyceraldehyde-3-phosphate dehydrogenase (GAPDH), and ribulose-1,5-bisphosphate carboxylase/oxygenase(Rubisco). Fructose-1,6-bisphosphatase (FBP), glyceraldehyde-3-phosphate dehydrogenase (GAPDH), and ribulose-1,5-bisphosphate carboxylase/oxygenase (Rubisco) play crucial roles in plant photosynthesis (Wu et al. 2025; Shin et al. 2024; Ge et al. 2020; Köhler et al. 2017). Among these, Rubisco is the rate-limiting enzyme in the Calvin cycle (Prywes et al. 2023; Rajarathinam et al. 2025). Two genes were differentially expressed for FBP and Rubisco, respectively, while one gene was differentially expressed for glyceraldehyde-3-phosphate dehydrogenase (GAPDH). Under BL exposure, the differentially expressed genes for these three enzymes were upregulated compared to other light conditions. This suggests that BL exposure promotes the enhancement of carbon assimilation efficiency within *D. salina* cells.

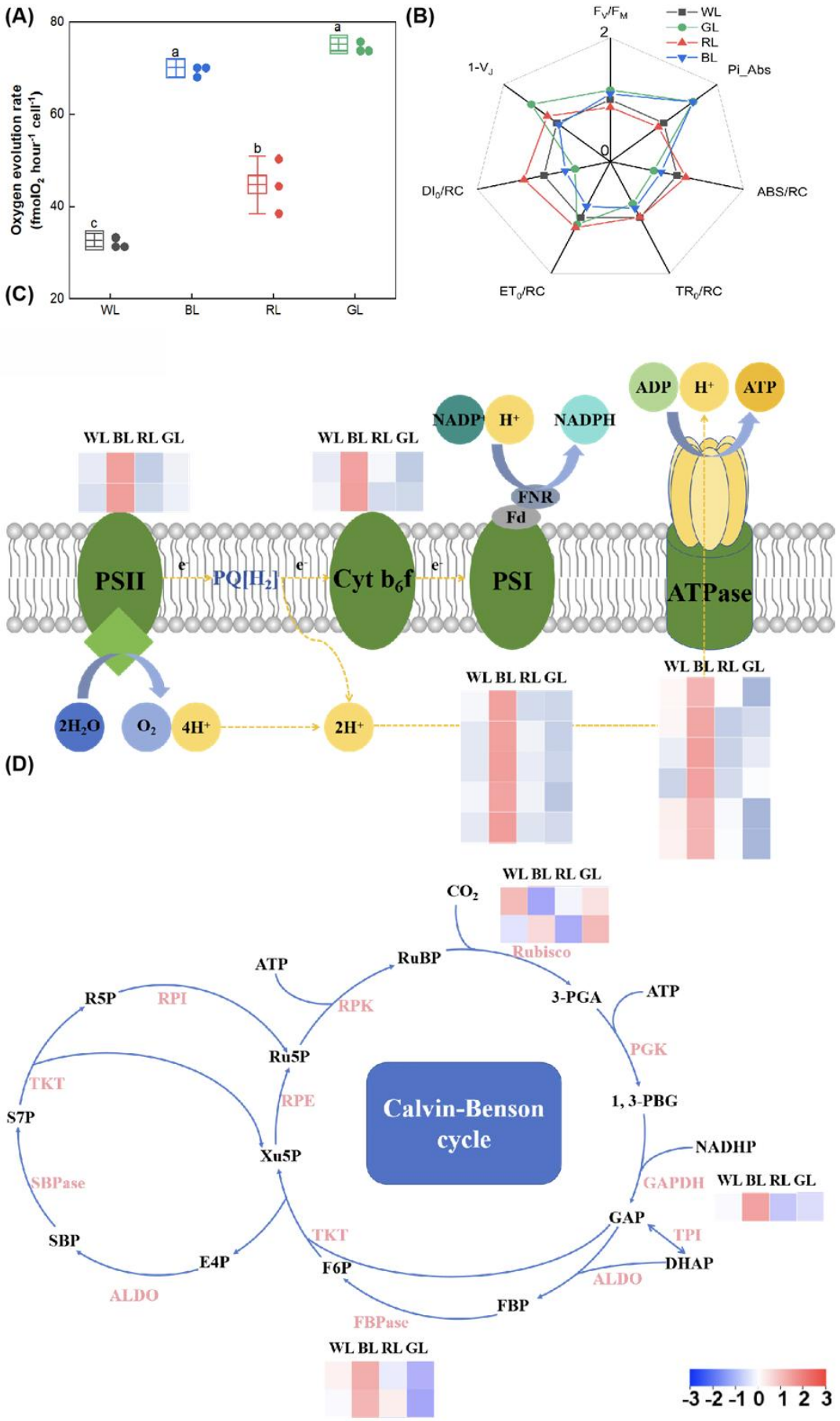

(A)
Oxygen evolution rate (fmolO_2 hour^{-1} cell^{-1})
80
60
40
20
a
b
c
WL
BL
RL
GL
(B)
F_V/F_M
2
0
WL
GL
RL
BL
Pi_Abs
ABS/RC
TR_0/RC
ET_0/RC
DI_0/RC
1-V_J
(C)
(D)
WL BL RL GL
PSII
PQ[H_2]
Cyt b_6f
PSI
ATPase
NADP$^+$
H^+
NADPH
FNR
Fd
ADP
H^+
ATP
e$^-$
2H_2O
O_2
4H^+
2H^+
CO_2
Rubisco
RuBP
3-PGA
ATP
PGK
1, 3-PBG
NADHP
GAPDH
GAP
TPI
DHAP
ALDO
FBP
FBPase
F6P
TKT
E4P
SBP
SBPase
S7P
TKT
Xu5P
RPE
Ru5P
RPK
ATP
R5P
RPI
Calvin-Benson cycle
-3 -2 -1 0 1 2 3

Fig. 6 Photosynthetic oxygen evolution rate of *Dunaliella salina* cultured for 50 days under blue (BL), red (RL), green (GL), and white light (WL) (**A**), chlorophyll a fluorescence transient parameters (**B**), a schematic diagram of the photosynthetic electron transport chain (**C**), and a schematic diagram of the relative changes in the Calvin cycle and differentially expressed genes (DEGs) (squares) under different light qualities (**D**). Data represent the mean ± SD of three biological replicates. Different letters (e.g., a and b) between treatment groups indicate significant differences ($P < 0.05$)

Effects of Light Quality on *Dunaliella* Respiration

After a 50-day cultivation period, the respiratory oxygen consumption rate, reactive oxygen species (ROS) levels, antioxidant enzyme activity, and gene expression levels in the oxidative phosphorylation (respiratory electron transport chain) pathway of *D. salina* were measured under different light quality conditions. As shown in Fig. 7A, the respiratory oxygen consumption rate of *D. salina* cells exposed to WL (26.72 ± 1.28 fmol $hour^{-1}$ $cell^{-1}$) was significantly higher than that under other light conditions. Analysis of ROS levels and antioxidant enzyme activity revealed significant differences in the effects of different light conditions on intracellular ROS levels and the degree of plasma membrane peroxidation in *D. salina* cells. The H_2O_2 content in *D. salina* cells exposed to WL (7.43 ± 0.04 nmol $(10^5$ cells$)^{-1}$) was significantly higher than that under RL exposure (6.14 ± 0.04 nmol $(10^5$ cells$)^{-1}$), BL exposure (3.85 ± 0.03 nmol $(10^5$ cells$)^{-1}$), and GL exposure (0.56 ± 0.04 nmol $(10^5$ cells$)^{-1}$) (Fig. 7B); The MDA content in *D. salina* cells exposed to WL (86.58 ± 1.63 pmol $(10^5$ cells$)^{-1}$) was significantly higher than the MDA content under RL exposure (51.37 ± 0.44 pmol $(10^5$ cells$)^{-1}$)), BL exposure (40.54 ± 0.01 pmol $(10^5$ cells$)^{-1}$)), and GL exposure (39.58 ± 6.04 pmol $(10^5$ cells$)^{-1}$)) (Fig. 7C); SOD activity in *D. salina* cells exposed to WL (0.87 ± 0.08 U $(10^5$ cells$)^{-1}$)) was significantly higher than that under RL exposure (0.70 ± 0.06 U $(10^5$ cells$)^{-1}$)), GL exposure (0.58 ± 0.01 U $(10^5$ cells$)^{-1}$)), and BL exposure (0.52 ± 0.01 U $(10^5$ cells$)^{-1}$)) (Fig. 7D); The APX activity of *D. salina* cells exposed to WL (7.30 ± 0.08 nmol min^{-1} $(10^5$ cells$)^{-1}$) was significantly higher than that under RL exposure (4.19 ± 0.18 nmol min^{-1} $(10^5$ cells$)^{-1}$), BL exposure (3.34 ± 0.33 nmol min^{-1} $(10^5$

cells)$^{-1}$), and GL exposure (1.68 ± 0.10 nmol min^{-1} (10^5 cells)$^{-1}$) (Fig. 7E). In summary, under WL exposure, the respiratory oxygen uptake rate, ROS content, and antioxidant enzyme activity of *D. salina* cells were significantly higher than under other light conditions, whereas under BL and GL exposure, the ROS content and antioxidant enzyme activity of *D. salina* cells were slightly lower than those under other light conditions. This indicates that WL exposure promotes the respiratory rate of *D. salina* and generates a large amount of ROS, thereby exacerbating the degree of peroxidation of the plasma membrane; whereas *D. salina* cells exposed to BL and GL produce less ROS and clear ROS more rapidly than those exposed to other light conditions.

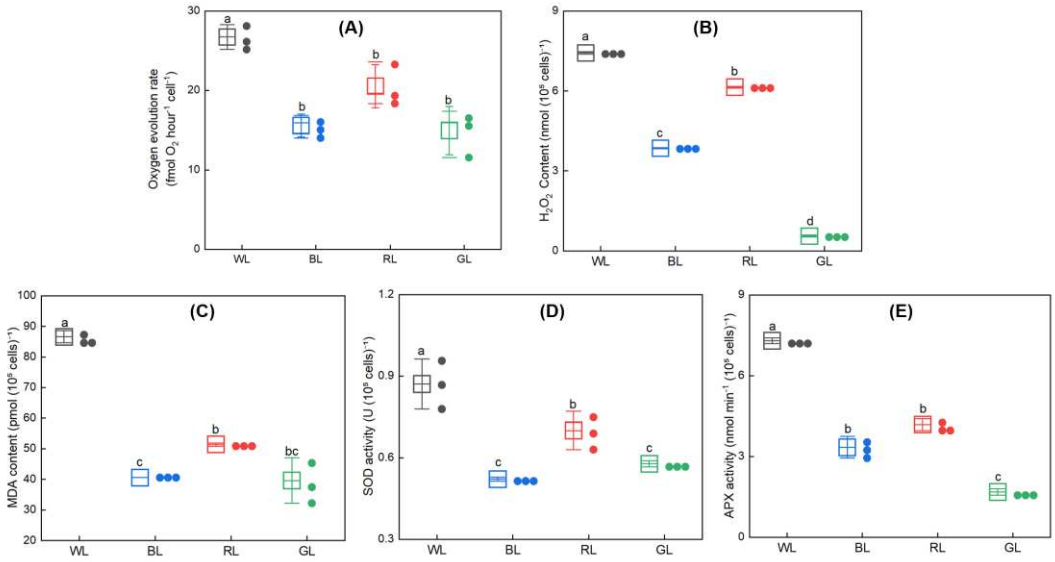


Fig. 7 Respiratory oxygen uptake rates (**A**), hydrogen peroxide (H_2O_2) content (**B**), malondialdehyde (MDA) content (**C**), superoxide dismutase (SOD) activity (**D**), and ascorbate peroxidase (APX) activity (**E**) of *Dunaliella salina* cultured for 50 days under blue light (BL), red light (RL), green light (GL), and white light (WL) gradients. Data represent the mean ± SD of three biological replicates. Different letters (e.g., a and b) between treatment groups indicate significant differences ($P < 0.05$)

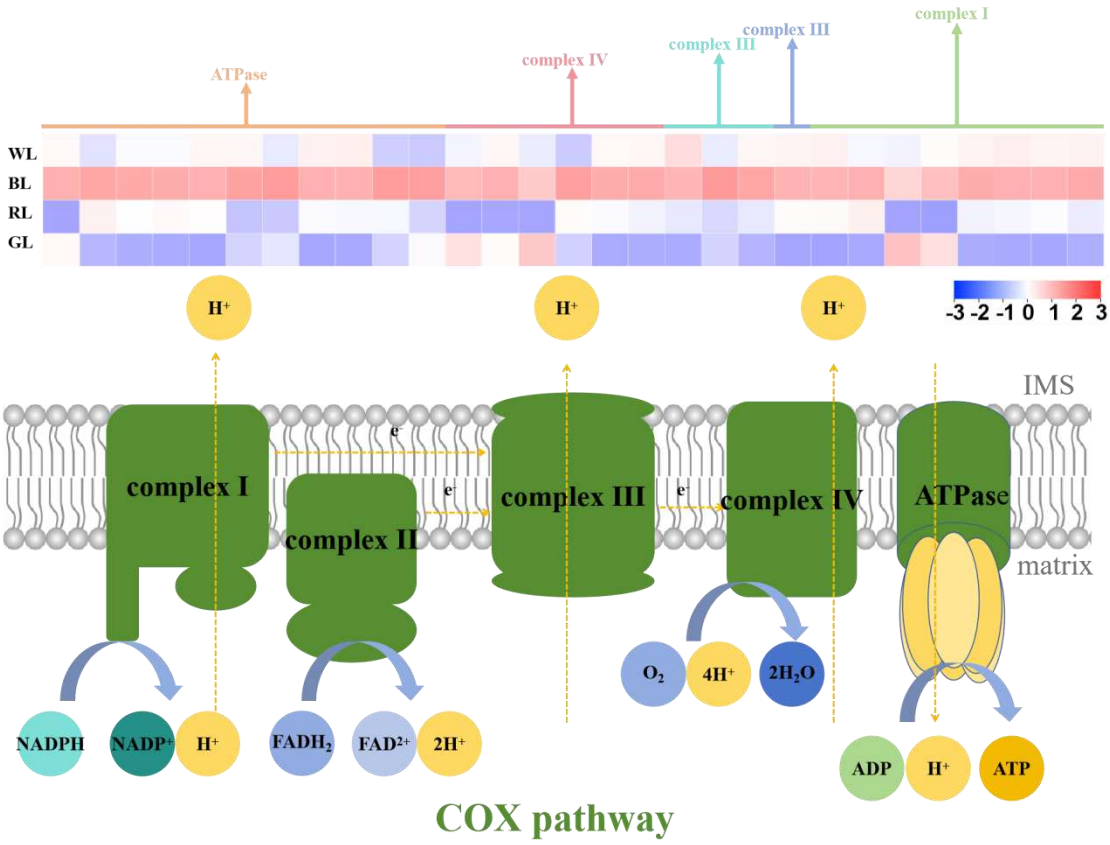
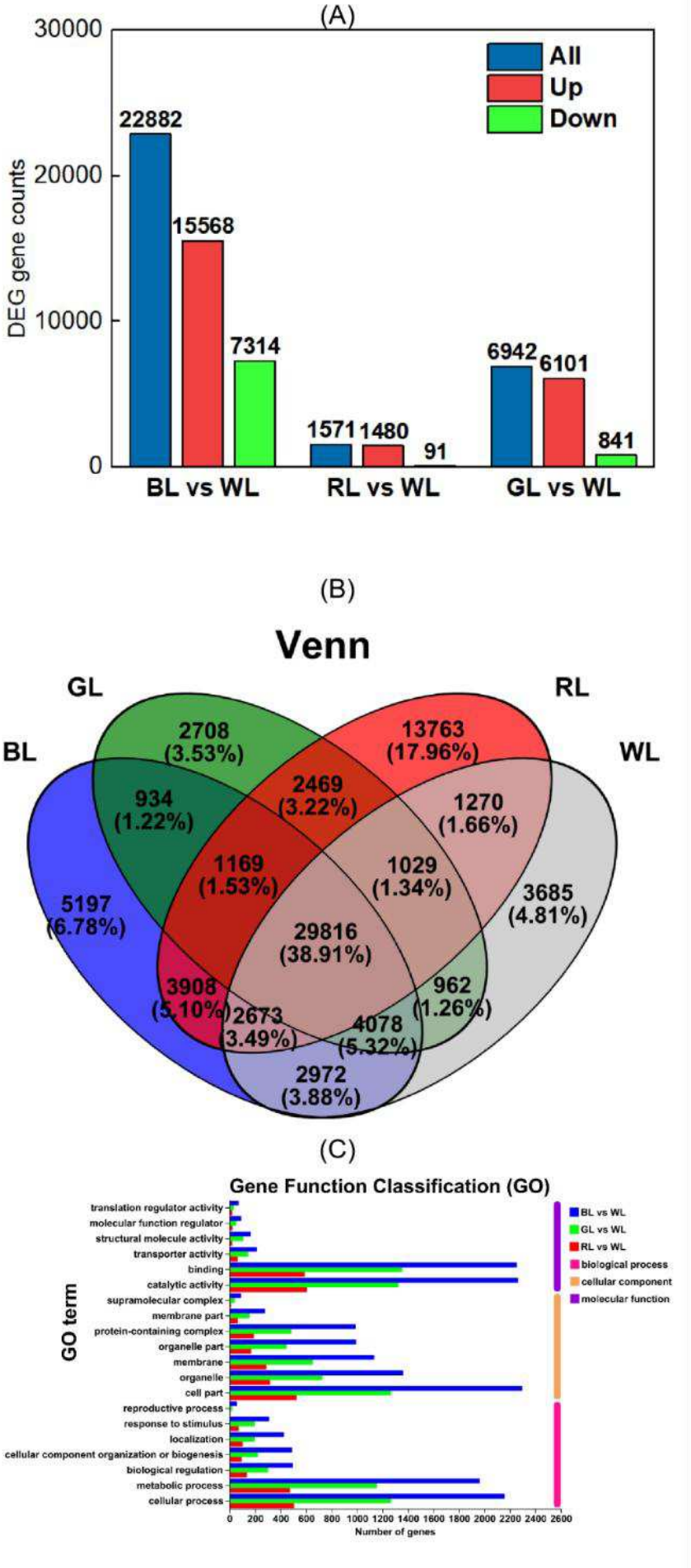


Fig. 8 Effects of gradient illumination with blue light (BL), red light (RL), green light (GL), and white light (WL) on genes involved in respiratory oxidative phosphorylation. Schematic diagram of the respiratory electron transport chain and DEG heatmap under different light quality conditions

Effects of Light Quality on Gene Expression in *Dunaliella salina*

In this study, a total of 76,633 differentially expressed genes (DEGs) were identified. As shown in Fig. 9A, the bar charts illustrate the number of differentially expressed genes, as well as the upregulated and downregulated genes, among treatment groups under different light conditions. The bar charts indicate that there were 22,882 differentially expressed genes between the BL and WL treatments, of which 15,568 were upregulated and 7,314 were downregulated; there were 1,571 differentially expressed genes between the RL and WL treatments, of which 1,480 were upregulated and 91 were downregulated; and 6,942 genes were differentially expressed between the GL and WL treatments, of which 6,101 were upregulated and 841 were downregulated. The transcriptomic Venn diagram shows that a total of 29,816 genes were differentially expressed under the four light quality conditions of BL, RL, WL, and GL (Fig. 8B). In

summary, the large number of differentially expressed genes indicates that light quality can significantly influence gene expression in *D. salina* cells. GO pathway enrichment analysis showed that DEGs were mainly enriched in the two functional categories of cellular components (CC) and molecular functions (MF) (Fig. 8C), indicating that light quality may primarily affect genes related to cellular composition and molecular functions in *D. salina* cells.


(A)
30000
20000
10000
0
DEG gene counts
All
Up
Down
22882
15568
7314
1571
1480
91
6942
6101
841
BL vs WL
RL vs WL
GL vs WL
(B)
Venn
GL
RL
BL
WL
2708 (3.53%)
13763 (17.96%)
934 (1.22%)
2469 (3.22%)
1270 (1.66%)
1169 (1.53%)
1029 (1.34%)
5197 (6.78%)
3685 (4.81%)
29816 (38.91%)
3908 (5.10%)
962 (1.26%)
2673 (3.49%)
4078 (5.32%)
2972 (3.88%)
(C)
Gene Function Classification (GO)
GO term
translation regulator activity
molecular function regulator
structural molecule activity
transporter activity
binding
catalytic activity
supramolecular complex
membrane part
protein-containing complex
organelle part
membrane
organelle
cell part
reproductive process
response to stimulus
localization
cellular component organization or biogenesis
biological regulation
metabolic process
cellular process
0 200 400 600 800 1000 1200 1400 1600 1800 2000 2200 2400 2600
Number of genes
BL vs WL
GL vs WL
RL vs WL
biological process
cellular component
molecular function

588 **Fig. 9** Gene expression levels in *Dunaliella salina* cells under blue light (BL), red light (RL), green
589 light (GL), and white light (WL) gradient illumination. Venn diagram of differentially expressed
590 genes (DEGs) in *D. salina* cells under BL, RL, WL, and GL treatments (**A**); Changes in differentially
591 expressed genes (DEGs) in *D. salina* cells under BL, RL, WL, and GL treatments (**B**); Gene
592 Ontology (GO) classification analysis of DEGs in *D. salina* cells under BL, RL, WL, and GL
593 treatments (**C**). DEGs can be classified into three functional categories: Biological Processes (BP),
594 Cellular Components (CC), and Molecular Functions (MF)

595 **Discussion**

596 Light quality is a key factor influencing algal cell proliferation, metabolism, and
597 biomass accumulation. The results indicate that monochromatic light quality can
598 modulate the expression levels of genes associated with photosynthesis and respiration
599 in *D. salina* cells, thereby affecting photosynthetic and respiratory efficiency and,
600 consequently, intracellular carbon allocation as well as biomass synthesis and
601 accumulation. *D. salina* cells exhibited the highest growth rates and dry weights under
602 BL exposure (Fig. 3). Most genes involved in photosynthetic phosphorylation, the
603 Calvin cycle, and oxidative phosphorylation were significantly upregulated under BL
604 (Fig. 6 and 8). This led to significant improvements in photosynthetic activity,
605 photosynthetic capacity, carbon assimilation efficiency, and reactive oxygen species
606 (ROS) scavenging capacity under BL (Fig. 6 and 7), thereby promoting the
607 accumulation and synthesis of chlorophyll, carotenoids (β-carotene), and proteins
608 within the algal cells (Fig. 4 and 5).

609 Previous studies have shown that high-light stress leads to the accumulation of
610 large amounts of carotenoids within *D. salina* cells (Ye et al. 2008). The orange
611 coloration and rounding of *D. salina* cells are manifestations of substantial carotenoid
612 accumulation within the algal cells (Kim et al. 2024). In this study, WL, RL, and BL at
613 an intensity of 200 μmol m^{-2} s^{-1} induced *D. salina* cells to enter the carotenoid
614 accumulation phase (Fig. 2). It has been reported that high-temperature stress can also
615 trigger carotenoid accumulation in *D. salina* (Gómez and González 2005), and the
616 experimental temperature of 30 ± 1 °C may have facilitated the rapid transition of *D.*

salina cells into the carotenoid accumulation phase. However, under GL, *D. salina* cells did not enter the yellow-cell stage but remained in the green-cell stage (Fig. 2). This difference may be associated with the relatively low light absorption capacity of *D. salina* for GL at the cellular and chloroplast levels (Li et al. 2020).

Under BL, the algal cell density and specific growth rate of *D. salina* were significantly superior to those under other light conditions. The highest specific growth rate was observed during the growth phase under medium light (ML, 100 ± 10 μmol m^{-2} s^{-1}), while under high light (HL, 200 ± 20 μmol m^{-2} s^{-1}) stress, algal cell density still maintained a certain degree of growth, whereas algal cells began to decrease under WL and RL (Fig. 3). This difference may be attributed to the higher respiratory efficiency observed under BL exposure (Fig. 8). Respiration provides the energy required for algal cell division and reproduction (Luo et al. 2025). Our results indicate that, in terms of light management strategies for the two-stage cultivation method, cultivating *D. salina* under BL conditions yields the optimal economic benefits.

Studies have reported that monochromatic light plays a positive role in the synthesis of cytochromes in *D. salina* (Nwoba et al. 2021). In this study, the results indicate that the chlorophyll content in *D. salina* cells exposed to BL remained at a high level during the high-light (HL, 200 ± 20 μmol m^{-2} s^{-1}) stress period, whereas the levels of carotenoids and β-carotene remained high during the medium-light (ML, 100 ± 10 μmol m^{-2} s^{-1}) growth phase and during the high-light (HL, 200 ± 20 μmol m^{-2} s^{-1}) stress period, compared to other light qualities (Fig. 4). These findings may be associated with the more efficient absorption of light energy by *D. salina* cells under BL and its subsequent transfer to the PSII reaction centers, where the absorbed energy can be more effectively utilized for carbon assimilation, thereby contributing to higher pigment contents and growth rates (Fig. 6). Carotenoid production, particularly that of β-carotene, is the most common strategy employed by most *Dunaliella* species under environmental stress (Jahnke and White 2003; Salguero et al. 2003). Since the production of β-carotene and other carotenoids is associated with oxygen consumption and ROS generation (Bennoun 2001; Xu and Harvey 2019), the increased levels of carotenoids and β-carotene under BL treatment can be interpreted as an indication of

enhanced ROS scavenging and oxygen consumption capacity in *D. salina*. This also explains why algal cells under blue light exhibit lower H_2O_2 and MDA levels, as well as lower SOD and APX activities (Fig. 7).

With regard to protein synthesis, Barro et al. (1989) reported that blue light (BL) promotes protein synthesis in terrestrial plants, such as soybeans. Studies have shown that blue light or a high proportion of blue light can promote protein synthesis in algae such as *Porphyra leucosticta* and *Chaetoceros* sp. (Korbee et al. 2005; del Pilar Sánchez-Saavedra and Voltolina 2006). This is consistent with our experimental results, which show that BL exposure increases protein content in *D. salina* cells (Fig. 5), a phenomenon that may be attributed to high protein turnover rates. Previous studies have reported changes in protein turnover in *D. salina* cells (Bahador et al. 2019; Mirshekari et al. 2019) and other higher plants (Hildebrandt et al. 2015; Huang and Jander 2017) under stress conditions. Protein turnover is a cellular phenomenon that regulates processes related to protein balance during stress, such as amino acid homeostasis, protein rearrangement, and the establishment of enzyme equilibrium (Hildebrandt 2018). Regarding glycerol synthesis, there were no significant differences in glycerol content within *D. salina* cells under BL, RL, and WL exposures, but the levels were higher than those under GL exposure (Fig. 5). The primary carbon source for glycerol synthesis in *D. salina* cells is photosynthesis rather than starch degradation. GL exposure can alter the allocation of carbon sources between starch and glycerol, which explains the higher starch content under GL exposure. Regarding starch and total lipids, previous studies have reported that red light can stimulate their synthesis and accumulation (Barro et al. 1989), which may act as a feedback regulation mechanism for photosynthesis (Hogewoning et al. 2010; Paul and Foyer 2001). This is consistent with our experimental results, in which RL exposure increased the starch and total lipid contents in *D. salina* cells (Fig. 5). This may be attributed to the fact that, under RL exposure, *D. salina* cells tend to synthesize and accumulate more carbohydrates as a means of protecting internal cellular structures in order to minimize damage caused by light stress (Jensen and Knutsen 1993).

Finally, a model was established to explain the differences in carbon supply and

677 allocation in *D. salina* cells under different light conditions (Fig. 10). The supply and
678 allocation of carbon fluxes under different light conditions were characterized based on
679 the expression patterns of differentially expressed genes (DEGs) involved in relevant
680 KEGG pathways. Photosynthesis is the primary source of carbon for *D. salina* cells
681 under different light conditions (Kim et al. 2024), Most DEGs in the photosynthesis
682 pathway (KO00195: Photosynthesis) were upregulated under BL exposure compared
683 to other light conditions. Under BL exposure, the photosynthetic electron transport
684 efficiency, carbon assimilation efficiency, and photosynthetic rate of *D. salina* were
685 significantly enhanced (Fig. 6), indicating that *D. salina* exposed to BL can assimilate
686 more carbon and incorporate it into the carbon pool compared to other light conditions.
687 Different light conditions have varying effects on carbon allocation and utilization in
688 *D. salina* cells. Under BL and GL exposure, most DEGs related to cell division
689 (GO0051301: Cell division) were upregulated compared to other light conditions. BL
690 exposure promotes cell proliferation and growth rate in *D. salina* (Fig. 3), indicating
691 that *D. salina* exposed to BL allocates more carbon flux to cell division than under other
692 light conditions. Under BL and GL exposure, most DEGs in the chlorophyll synthesis
693 pathway (KO00900: Terpenoid backbone biosynthesis) were upregulated compared to
694 other light conditions. BL and GL exposure further promoted chlorophyll synthesis and
695 accumulation in *D. salina* cells (Fig. 4A), indicating that *D. salina* cells under BL and
696 GL exposure allocated more carbon flux to chlorophyll synthesis than under other light
697 conditions. Under BL exposure, most differentially expressed genes (DEGs) involved
698 in the protein export pathway (KO03060) in *D. salina* cells were upregulated compared
699 with other light conditions, which indicates that BL may facilitate protein targeting and
700 transmembrane transport. Combined with the higher protein content observed under BL
701 exposure, these findings indicate that BL favors protein accumulation in *D. salina* cells
702 (Fig. 5). This indicates that *D. salina* exposed to BL allocate more carbon flux to protein
703 synthesis than those exposed to other light conditions. Under RL exposure, most DEGs
704 in the starch metabolism pathway (KO00500: Starch and sucrose metabolism) of
705 *D. salina* cells were upregulated compared to other light conditions, indicating that RL
706 exposure promotes starch synthesis and accumulation in *D. salina* cells (Fig. 5). This

suggests that *D. salina* cells exposed to RL allocate more carbon flux to starch synthesis than those exposed to other light conditions. Most DEGs in the glycerolipid metabolism pathway (KO00561) of *D. salina* cells exposed to RL and WL were upregulated compared to other light conditions. *D. salina* cells exposed to RL and WL were able to synthesize and accumulate more glycerol than those exposed to GL (Fig. 5), indicating that *D. salina* cells exposed to RL and WL allocate more carbon flux to glycerol synthesis than those exposed to other light conditions. Most DEGs in the total lipid synthesis pathway (KO00061: Fatty acid biosynthesis) of *D. salina* cells exposed to RL were upregulated compared to other light conditions. RL exposure promotes the synthesis and accumulation of fatty acids (total lipids) in *D. salina* cells (Fig. 5), indicating that *D. salina* cells exposed to RL allocate more carbon flux to fatty acid (total lipid) synthesis than those exposed to other light conditions. Finally, the mechanisms underlying differences in carbon supply, allocation, and utilization in *D. salina* cells exposed to different light conditions were elucidated based on differential gene expression and physiological and biochemical metabolism (Fig. 10).

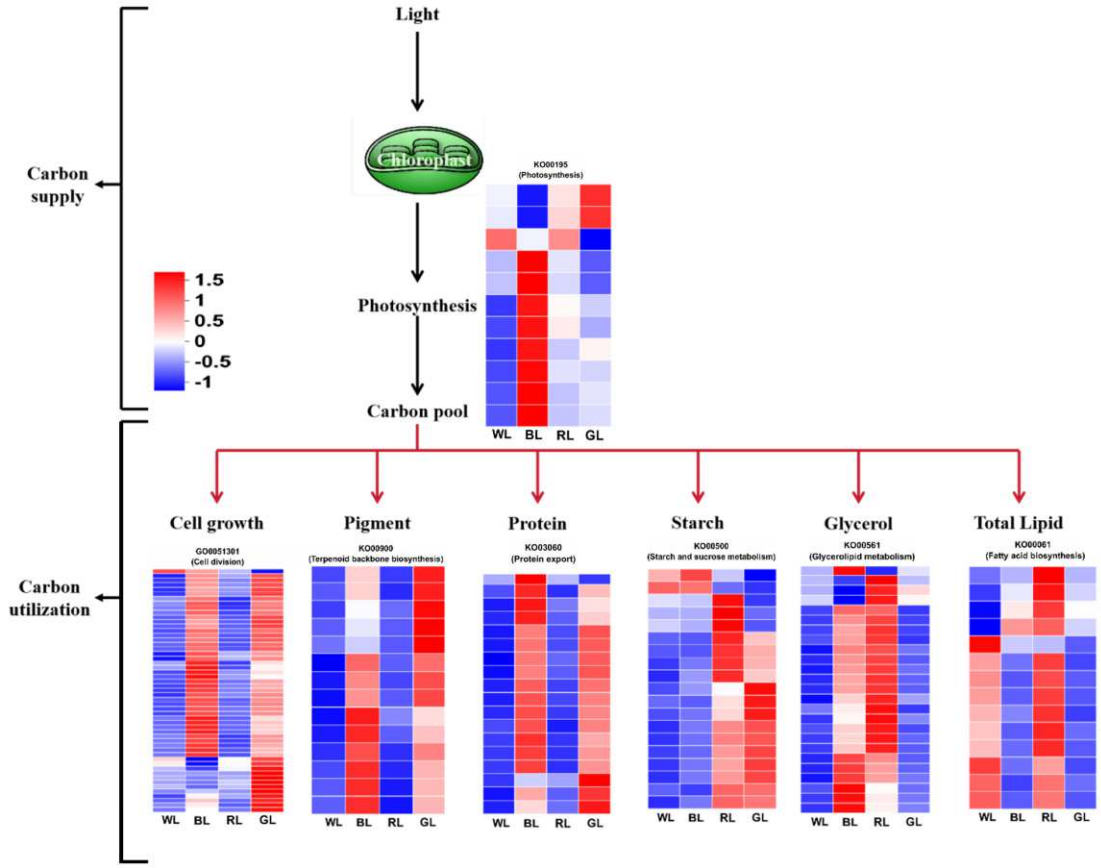


Fig.10 Schematic illustration of differences in carbon allocation in *Dunaliella salina* cells under

blue light (BL), red light (RL), green light (GL), and white light (WL) gradients. Under different light conditions, the primary carbon source for *D. salina* cells comes from photosynthesis (KO00195: Photosynthesis). The carbon pool formed through photosynthetic pathways is allocated to *D. salina* for cell division (GO0051301: Cell division), pigment synthesis (KO00900: Terpenoid backbone biosynthesis), protein export (KO03060: Protein export), starch metabolism (KO00500: Starch and sucrose metabolism), glycerol metabolism (KO00561: Glycerolipid metabolism), and total lipid synthesis (KO00061: Fatty acid biosynthesis). Black arrows represent the transfer of light energy from the chloroplasts of *D. salina* cells to the carbon pool via photosynthesis, while red arrows indicate the direction of carbon flux distribution

Conclusion

Exposure to blue light (BL) is more conducive to the proliferation and division of *D. salina* cells, as well as the synthesis of pigments (chlorophyll and carotenoids) and proteins, compared to exposure to other light qualities. This is primarily attributed to the fact that, under BL exposure, *D. salina* cells exhibit higher photosynthetic electron transport efficiency, carbon assimilation efficiency, photosynthetic activity, respiratory electron transport efficiency, and reactive oxygen species scavenging rates. Starch accumulation was the highest in *D. salina* cells exposed to red light (RL), whereas total lipid accumulation was greater under white light (WL) and RL exposure. These differences may be associated with light-quality-dependent variations in oxidative stress and carbon metabolic allocation, suggesting that the accumulation of starch and lipids may represent an adaptive physiological response of *D. salina* cells to changes in light quality and oxidative stress.

Light quality can regulate the upstream supply and downstream distribution of carbon flux within *D. salina* cells, thereby controlling algal growth, reproduction, and the accumulation and synthesis of biomass. First, light quality regulates photosynthetic electron transport efficiency, carbon assimilation efficiency, and photosynthetic rate by influencing gene expression levels in photosynthetic pathways such as the photosynthetic electron transport chain and the Calvin cycle, thereby controlling the supply of carbon flux. This represents the regulatory role of light quality on the

upstream supply of carbon flux in *D. salina*. Subsequently, light quality regulates the allocation of carbon flux by influencing gene expression levels in biomass synthesis pathways (such as terpenoid biosynthesis, protein processing in the endoplasmic reticulum, starch and sucrose metabolism, glycerol ester metabolism, and fatty acid biosynthesis), thereby controlling algal cell growth, reproduction, and biomass synthesis.

Authors' contribution Jiale Gu: Methodology, Validation. Yongfu Li: Conceptualization, Investigation, Data curation, Writing-review. Tianze Zhao: Conceptualization, Supervision, Validation, Writing-review. Delong Li: Writing-review. Xingkai Che: Investigation, Writing-editing. Ruiqian Li: Methodology, Conceptualization, Supervision.

Funding This work was supported by the National Natural Science Foundation of China (No. 42576109).

Data availability Data will be made available on request.

Declarations

The authors declare no competing interests.

References

Araj-Shirvani M, Honarvar M, Jahadi M, Mizani M (2024) Biochemical profile of *Dunaliella* isolates from different regions of Iran with a focus on pharmaceutical and nutraceutical potential applications. Food Sci Nutr 12:4914–4926

Arnon DI (1949) Copper enzymes in isolated chloroplasts. Polyphenoloxidase in *Beta vulgaris*. Plant Physiol 24:1–15

Aziz MMA, Kassim KA, Shokravi Z, Jakarni FM, Liu HY, Zaini N, Tan LS, Islam ABMS, Shokravi H (2020) Two-stage cultivation strategy for simultaneous increases in growth rate and lipid content of microalgae: a review. Renew Sustain Energy Rev 119:109621

779 Bahador E, Einali A, Azizian-Shermeh O, Sangtarash MH (2019) Metabolic responses
780 of the green microalga *Dunaliella salina* to silver nanoparticles-induced oxidative
781 stress in the presence of salicylic acid treatment. Aquat Toxicol 217:105356

782 Bamary Z, Einali A (2022) Changes in carbon partitioning and pattern of antioxidant
783 enzyme activity induced by arginine treatment in the green microalga *Dunaliella*
784 *salina* under long-term salinity. Microb Ecol 84:198–212

785 Barro F, De La Haba P, Maldonado JM, Fontes AG (1989) Effect of light quality on
786 growth, contents of carbohydrates, protein and pigments, and nitrate reductase
787 activity in soybean plants. J Plant Physiol 134:586–591

788 Ben-Amotz A (1995) New mode of *Dunaliella* biotechnology: two-phase growth for β-
789 carotene production. J Appl Phycol 7:65–68

790 Ben-Amotz A, Avron M (1983) On the factors which determine massive β-carotene
791 accumulation in the halotolerant alga *Dunaliella bardawil*. Plant Physiol 72:593–
792 597

793 Ben-Amotz A, Katz A, Avron M (1982) Accumulation of β-carotene in halotolerant
794 algae: purification and characterization of β-carotene-rich globules from *Dunaliella*
795 *bardawil* (Chlorophyceae). J Phycol 18:529–537

796 Bennoun P (2001) Chlororespiration and the process of carotenoid biosynthesis.
797 Biochim Biophys Acta Bioenerg 1506:133–142

798 Beyer WF Jr, Fridovich I (1987) Assaying for superoxide dismutase activity: some
799 large consequences of minor changes in conditions. Anal Biochem 161:559–566

800 Bligh EG, Dyer WJ (1959) A rapid method of total lipid extraction and purification.
801 Can J Biochem Physiol 37:911–917

802 Borowitzka LJ, Borowitzka MA (1989) β-Carotene (provitamin A) production with
803 algae. In: Vandamme EJ (ed) Biotechnology of vitamins, pigments and growth
804 factors. Springer, Dordrecht, pp 15–26

805 Borowitzka MA (1988) Algal growth media and sources of algal cultures. In:
806 Borowitzka MA, Borowitzka LJ (eds) Micro-algal biotechnology. Cambridge
807 University Press, Cambridge, pp 456–465

808 Borowitzka MA (2013) *Dunaliella*: biology, production, and markets. In: Richmond A,
809 Hu Q (eds) Handbook of microalgal culture: applied phycology and biotechnology,
810 2nd edn. Wiley-Blackwell, Oxford, pp 359–368

Bradford MM (1976) A rapid and sensitive method for the quantitation of microgram quantities of protein utilizing the principle of protein-dye binding. Anal Biochem 72:248–254

Chen D, Li Z, Shi J, Suen H, Zheng X, Zhang C, Xue T (2024) Genomics and transcriptomics reveal β-carotene synthesis mechanism in *Dunaliella salina*. Front Microbiol 15:1389224

Chen H, Jiang JG, Wu GH (2009) Effects of salinity changes on the growth of *Dunaliella salina* and its isozyme activities of glycerol-3-phosphate dehydrogenase. J Agric Food Chem 57:6178–6182

Chen S, Li X, Ma X, Qing R, Chen Y, Zhou H, Yu Y, Li J, Tan Z (2023) Lighting the way to sustainable development: physiological response and light control strategy in microalgae-based wastewater treatment under illumination. Sci Total Environ 903:166298

Chin GJWL, Andrew AR, Abdul-Sani ER, Yong WTL, Misson M, Anton A (2023) The effects of light intensity and nitrogen concentration to enhance lipid production in four tropical microalgae. Biocatal Agric Biotechnol 48:102660

Danesh AF, Ebrahimi S, Salehi A, Parsa A (2017) Impact of nutrient starvation on intracellular biochemicals and calorific value of mixed microalgae. Biochem Eng J 125:56–64

Debnath S, Muthuraj M, Bandyopadhyay TK, Bobby MN, Vanitha K, Tiwari ON, Bhunia B (2024) Engineering strategies and applications of cyanobacterial exopolysaccharides: a review on past achievements and recent perspectives. Carbohydr Polym 328:121686

Del-Campo JA, García-González M, Guerrero MG (2007) Outdoor cultivation of microalgae for carotenoid production: current state and perspectives. Appl Microbiol Biotechnol 74:1163–1174

Esteves AF, Gonçalves AL, Vilar VJ, Pires JC (2024) Comparative assessment of microalgal growth kinetic models based on light intensity and biomass concentration. Bioresour Technol 394:130167

Ferguson IB, Watkins CB, Harman JE (1983) Inhibition by calcium of senescence of detached cucumber cotyledons: effect on ethylene and hydroperoxide production. Plant Physiol 71:182–186

Ge Q, Cui Y, Li J, Gong J, Lu Q, Li P, Gong W (2020) Disequilibrium evolution of the Fructose-1, 6-bisphosphatase gene family leads to their functional biodiversity in *Gossypium* species. BMC Genomics 21:20

Guermazi W, Masmoudi S, Trabelsi NA, Gammoudi S, Ayadi H, Morant-Manceau A, Hotos GN (2023) Physiological and biochemical responses in microalgae *Dunaliella salina*, *Cylindrotheca closterium* and *Phormidium versicolor* NCC466 exposed to high salinity and irradiation. Life 13:313

Heath RL, Packer L (1968) Photoperoxidation in isolated chloroplasts: I. Kinetics and stoichiometry of fatty acid peroxidation. Arch Biochem Biophys 125:189–198

Hildebrandt TM (2018) Synthesis versus degradation: directions of amino acid metabolism during *Arabidopsis* abiotic stress response. Plant Mol Biol 98:121–135

Hildebrandt TM, Nesi AN, Araújo WL, Braun HP (2015) Amino acid catabolism in plants. Mol Plant 8:1563–1579

Hogewoning SW, Trouwborst G, Maljaars H, Poorter H, van Ieperen W, Harbinson J (2010) Blue light dose–responses of leaf photosynthesis, morphology, and chemical composition of *Cucumis sativus* grown under different combinations of red and blue light. J Exp Bot 61:3107–3117

Huang T, Jander G (2017) Abscisic acid-regulated protein degradation causes osmotic stress-induced accumulation of branched-chain amino acids in *Arabidopsis thaliana*. Planta 246:737–747

Jahnke LS, White AL (2003) Long-term hyposaline and hypersaline stresses produce distinct antioxidant responses in the marine alga *Dunaliella tertiolecta*. J Plant Physiol 160:1193–1202

Jensen S, Knutsen G (1993) Influence of light and temperature on photoinhibition of photosynthesis in *Spirulina platensis*. J Appl Phycol 5:495–504

Jin Y, Li Y, Qi Y, Wei Q, Yang G, Ma X (2024) A modified cultivation strategy to enhance biomass production and lipid accumulation of *Tetradesmus obliquus* FACHB-14 with copper stress and light quality induction. Bioresour Technol 400:130677

Kim DG, Lee C, Park SM, Choi YE (2014) Manipulation of light wavelength at appropriate growth stage to enhance biomass productivity and fatty acid methyl ester yield using *Chlorella vulgaris*. Bioresour Technol 159:240–248

Kim M, Kim J, Lee S, Khanh N, Li Z, Polle JE, Jin E (2024a) Deciphering the β-carotene hyperaccumulation in *Dunaliella* by the comprehensive analysis of *Dunaliella salina* and *Dunaliella tertiolecta* under high light conditions. Plant Cell Environ 47:213–229

879 Kim M, Kim Y, Lee JW, Jin E, Kim GH (2024b) Second stage of β-carotene
880 biosynthesis under high light in *Dunaliella salina* is regulated by NADPH oxidase
881 homologs. Algal Res 78:103416

882 Köhler IH, Ruiz-Vera UM, VanLoocke A, Thomey ML, Clemente T, Long SP,
883 Bernacchi CJ (2017) Expression of cyanobacterial FBP/SBPase in soybean
884 prevents yield depression under future climate conditions. J Exp Bot 68:715–726

885 Korbee N, Figueroa FL, Aguilera J (2005) Effect of light quality on the accumulation
886 of photosynthetic pigments, proteins and mycosporine-like amino acids in the red
887 alga *Porphyra leucosticta* (Bangiales, Rhodophyta). J Photochem Photobiol B
888 80:71–78

889 Kumar V, Bhoyar MS, Mohanty CS, Chauhan PS, Toppo K, Ratha SK (2024)
890 Untapping the potential of algae for β-glucan production: a review of biological
891 properties, strategies for enhanced production and future perspectives. Carbohydr
892 Polym 348:122895

893 Lam MK, Lee KT (2014) Scale-up and commercialization of algal cultivation and
894 biofuel production. In: Pandey A, Lee DJ, Chisti Y, Soccol C (eds) Biofuels from
895 algae. Elsevier, Amsterdam, pp 261–286

896 Lamers PP, Janssen M, De Vos RC, Bino RJ, Wijffels RH (2008) Exploring and
897 exploiting carotenoid accumulation in *Dunaliella salina* for cell-factory
898 applications. Trends Biotechnol 26:631–638

899 Lan Y, Song Y, Guo Y, Qiao D, Cao Y, Xu H (2022) DsLCYB directionally modulated
900 β-carotene of the green alga *Dunaliella salina* under red light stress. J Microbiol
901 Biotechnol 32:1622–1631

902 Li D, Li Y, Li R, Che X, Wang L, Zhang A, Liu J, Ma D (2026) Light quality regulation
903 of microalgal growth and metabolite accumulation: photophysiology, molecular
904 mechanisms, and machine learning insights. Aquaculture 627:744560

905 Li Q, Tan L, Wang J (2024) Single and combined toxic effects of nCu and nSiO2 on
906 *Dunaliella salina*. Environ Sci Pollut Res 31:30256–30268

907 Li Y, Li L, Liu J, Qin R (2020) Light absorption and growth response of *Dunaliella*
908 under different light qualities. J Appl Phycol 32:1041–1052

909 Li Y, Zhao T, Qin M, Che X, Zhang A (2024) Toxicity of the sunscreen UV filter
910 benzophenone-3 (OBZ) to the microalga *Selenastrum capricornutum*: an insight
911 into OBZ's damage to photosynthesis and respiration. Ecotoxicol Environ Saf
912 278:116441

913 Liu D, Yang W, Lv Y, Li S, Qv M, Dai D, Zhu L (2023) Pollutant removal and toxic
914 response mechanisms of freshwater microalgae *Chlorella sorokiniana* under
915 exposure of tetrabromobisphenol A and cadmium. Chem Eng J 461:142065

916 Luo J, Huang Y, Lai J, Liang J, Luo X, Li C, Zhao M (2025) Effects of tritium pollution
917 on photosynthesis, respiration and redox of microalgae under rising temperature.
918 Sci Total Environ 958:177766

919 Mirshekari M, Einali A, Valizadeh J (2019) Metabolic changes and activity pattern of
920 antioxidant enzymes induced by salicylic acid treatment in green microalga
921 *Dunaliella salina* under nitrogen deficiency. J Appl Phycol 31:1709–1719

922 Mirzaie MM, Lak ZJ, Meybodi FH (2021) A new shifting strategy in flashing light
923 based on the cell growth curve to enhance β-carotene biosynthesis in *Dunaliella*
924 *salina*. Curr Microbiol 78:2733–2740

925 Mohanta A, Prasad N, Khadim SR, Singh P, Singh S, Singh A, Asthana RK (2024)
926 Optimizing light regimes for neutral lipid accumulation in *Dunaliella salina* MCC
927 43: a study on physiological status and carbon allocation. World J Microbiol
928 Biotechnol 40:82

929 Mohebi Najafabadi M, Naeimpoor F (2023) Boosting β-carotene and storage materials
930 productivities by two-stage mixed and monochromatic exposure stresses on
931 *Dunaliella salina*. Int J Phytoremediation 25:609–620

932 Moheimani NR, Parlevliet D (2013) Sustainable solar energy conversion to chemical
933 and electrical energy. Renew Sustain Energy Rev 27:494–504

934 Mu N, Mehar JG, Mudliar SN, Shekh AY (2019) Recent advances in microalgal
935 bioactives for food, feed, and healthcare products: commercial potential, market
936 space, and sustainability. Compr Rev Food Sci Food Saf 18:1882–1897

937 Nwoba EG, Rohani T, Raeisossadati M, Vadiveloo A, Bahri PA, Moheimani NR (2021)
938 Monochromatic light filters to enhance biomass and carotenoid productivities of
939 *Dunaliella salina* in raceway ponds. Bioresour Technol 340:125689

940 Oldenhof H, Zachleder V, Van Den Ende H (2006) Blue- and red-light regulation of
941 the cell cycle in *Chlamydomonas reinhardtii* (Chlorophyta). Eur J Phycol 41:313–
942 320

943 Pais R, Conde T, Neves BB, Pinho M, Coelho M, Pereira H, Melo T (2024) Bioactive
944 lipids in *Dunaliella salina*: implications for functional foods and health. Foods
945 13:3321

946 Paul MJ, Foyer CH (2001) Sink regulation of photosynthesis. J Exp Bot 52:1383–1400

Prieto A, Cañavate JP, García-González M (2011) Assessment of carotenoid production by *Dunaliella salina* in different culture systems and operation regimes. J Biotechnol 151:180–185

Priscilla K, Sharma V, Gautam A, Gupta P, Dagar R, Kishore V, Kumar R (2024) Carotenoid extraction from plant tissues. In: Reddy YS (ed) Plant functional genomics: methods and protocols, vol 2. Springer US, New York, pp 3–18

Prywes N, Phillips NR, Tuck OT, Valentin-Alvarado LE, Savage DF (2023) Rubisco function, evolution, and engineering. Annu Rev Biochem 92:385–410

Qin R, Li Y, Zhang L, Liu J (2021) The effect of salinity shock on the growth and rapid light curve of *Dunaliella salina*. Aquac Res 52:2569–2579

Rajarathinam Y, Wittemeier L, Gutekunst K, Hagemann M, Kopka J (2025) Dynamic photosynthetic labeling and carbon-positional mass spectrometry monitor in vivo Rubisco carbon assimilation rates. Plant Physiol 197:kiaf020

Saini DK, Chakdar H, Pabbi S, Shukla P (2020) Enhancing production of microalgal biopigments through metabolic and genetic engineering. Crit Rev Food Sci Nutr 60:391–405

Salguero A, de la Morena B, Vigara J, Vega JM, Vilchez C, León R (2003) Carotenoids as protective response against oxidative damage in *Dunaliella bardawil*. Biomol Eng 20:249–253

Sánchez-Saavedra MP, Voltolina D (2006) The growth rate, biomass production and composition of *Chaetoceros* sp. grown with different light sources. Aquac Eng 35:161–165

Shin SE, Koh HG, Park K, Park SH, Chang YK, Kang NK (2024) Increasing lipid production in *Chlamydomonas reinhardtii* through genetic introduction for the overexpression of glyceraldehyde-3-phosphate dehydrogenase. Front Bioeng Biotechnol 12:1396127

Singh P, Singh S, Maurya P, Mohanta A, Dubey H, Khadim SR, Asthana RK (2023) Bioaccumulation of selenium in halotolerant microalga *Dunaliella salina* and its impact on photosynthesis, reactive oxygen species, antioxidative enzymes, and neutral lipids. Mar Pollut Bull 190:114842

Singh U, Laxmi, Singh P, Singh AK, Singh S, Kumar D, Asthana RK (2023) In silico and in vitro evaluation of extract derived from *Dunaliella salina*, a halotolerant microalga for its antifungal and antibacterial activity. J Biomol Struct Dyn 41:7069–7083

Strasser B, Strasser R (1995) Measuring fast fluorescence transients to address environmental questions: the JIP test. In: Mathis P (ed) Photosynthesis: from light to biosphere. Kluwer Academic Publishers, Dordrecht, pp 977–980

Strasser RJ, Tsimilli-Michael M, Srivastava A (2004) Analysis of the chlorophyll a fluorescence transient. In: Papageorgiou GC, Govindjee (eds) Chlorophyll a fluorescence: a signature of photosynthesis. Springer, Dordrecht, pp 321–362

Sui Y, Mazzucchi L, Acharya P, Xu Y, Morgan G, Harvey PJ (2021) A comparison of β-carotene, phytoene and amino acids production in *Dunaliella salina* DF 15 (CCAP 19/41) and *Dunaliella salina* CCAP 19/30 using different light wavelengths. Foods 10:2824

Thangsiri S, Inthachat W, Temviriyanukul P, Sahasakul Y, Trisonthi P, Pan-Utai W, Suttisansanee U (2024) Bioactive compounds and in vitro biological properties of *Arthrospira platensis* and *Arthrospira maxima*: a comparative study. Sci Rep 14:23786

Ueno Y, Aikawa S, Kondo A, Akimoto S (2019) Adaptation of light-harvesting functions of unicellular green algae to different light qualities. Photosynth Res 139:145–154

Wu T, Tissue DT, Jiang M, Slot M, Crous KY, Yuan J, Mao R (2025) Leaf photosynthetic and respiratory thermal acclimation in terrestrial plants in response to warming: a global synthesis. Glob Chang Biol 31:e70026

Xi Y, Xue S, Cao X, Chi Z, Wang J (2021) Quantitative analysis on photon numbers received per cell for triggering β-carotene accumulation in *Dunaliella salina*. Bioresour Bioprocess 8:104

Xu Y, Harvey PJ (2019) Carotenoid production by *Dunaliella salina* under red light. Antioxidants 8:123

Xue J, Wang L, Zhang L, Balamurugan S, Li DW, Zeng H, Li HY (2016) The pivotal role of malic enzyme in enhancing oil accumulation in green microalga *Chlorella pyrenoidosa*. Microb Cell Fact 15:120

Ye ZW, Jiang JG, Wu GH (2008) Biosynthesis and regulation of carotenoids in *Dunaliella*: progresses and prospects. Biotechnol Adv 26:352–360

Yu C, Hu Y, Zhang Y, Luo W, Zhang J, Xu P, Shao S (2024) Concurrent enhancement of biomass production and phycocyanin content in salt-stressed *Arthrospira platensis*: a glycine betaine-supplementation approach. Chemosphere 353:141387

Yu S, Xu C, Tang T, Zhang Y, Effiong K, Hu J, Xiao X (2023) Down-regulation of iron/zinc ion transport and toxin synthesis in *Microcystis aeruginosa* exposed to 5,4′-dihydroxyflavone. J Hazard Mater 460:132396

Zhang LT, Zhang ZS, Gao HY, Xue ZC, Yang C, Meng XL, Meng QW (2011) Mitochondrial alternative oxidase pathway protects plants against photoinhibition by alleviating inhibition of the repair of photodamaged PSII through preventing formation of reactive oxygen species in *Rumex* K-1 leaves. Physiol Plant 143:396–407

Zhang P, Xin Y, He Y, Tang X, Shen C, Wang Q, Xu J (2022) Exploring a blue-light-sensing transcription factor to double the peak productivity of oil in *Nannochloropsis oceanica*. Nat Commun 13:1664

Zhao T, Li Y, Che X, Qin M, Zhang A, Wang J (2025) Effects of monochromatic LED light quality on photosynthetic capacity and pigment content in *Dunaliella salina* under low light intensity. J Appl Phycol 37:1719–1734